Russian Chemical Reviews **81** (2) 105 – 129 (2012) © 2012 Russian Academy of Sciences and Turpion Ltd

DOI 10.1070/RC2012v081n02ABEH004213

Structural studies of crystals of organic and organoelement compounds using modern quantum chemical calculations within the framework of the density functional theory

A A Korlyukov, M Yu Antipin

Contents

I.	Introduction	105
II.	DFT functionals, basis sets and pseudopotentials	106
III.	The software: a brief survey	108
IV.	The accuracy of calculations, reproduction of unit cell parameters and taking account of the van der Waals correction	109
V.	Studies of the relative stability of polymorphs	111
VI.	Studies of the electronic structure	113
VII.	Topological analysis of the calculated electron density of crystals	114
VIII.	Estimates of NMR and EPR spectroscopic characteristics	119
IX.	Parameters of vibrational spectra	121
X.	Dynamic processes in crystals	124
XI.	Refinement of structural models used in powder X-ray diffraction	125

Abstract. The review generalizes the results of structural studies of crystals of organic and organometallic compounds by modern quantum chemical calculations within the framework of the density functional theory reported in the last decade. Features of the software for such calculations are discussed. Examples of the use of quantum chemical calculations for the studies of the electronic structure, spectroscopic and other physicochemical properties of molecular crystals are presented. The bibliography includes 223 references.

I. Introduction

Investigations of the electronic structure of crystals and interfaces by the computational methods based on the density functional theory (DFT) is the most important tool of analysis of the properties of substances and materials. Quantum chemical calculations with periodic boundary conditions are usually carried out by researchers working in the field of physics of condensed media. The number of publications in this field is very high and shows a stable trend towards further increase. Until recently, similar calculations of structure of crystals within the framework of DFT were mainly performed for rather simple inorganic compounds and materials often treated as model systems. However, modern level of development of theory and computational tools allows one to go to quantum chemical calculations of crystals of more complex (organic and organoelement) compounds. This makes DFT calculations more important in studies of the structure of molecular compounds. It should be noted that such calculations (even the simplest ones) are used rarely in crystal chemistry of organic and organoelement compounds. Seemingly, they could make it possible to study the molecular and electronic structures of molecules in more detail compared to quantum chemical calculations of isolated molecules or molecular aggregates (clusters), especially when the effect of crystal packing on the properties of matter is taken into account. Nevertheless, for some reasons quantum chemical calculations of molecular crystals of organic and organoelement compounds still remain of limited use.

This situation is to a great extent due to the lack of experience by many crystallographers working in the field of rapidly progressing computational solid state physics. Also, this precludes active use of software and correct interpretation of results. The available methodological literature is mainly suitable for domain specialists in DFT. Software packages developed to study molecular systems without using periodic boundary conditions, *i.e.*, to carry out calculations of isolated molecules or their aggregates (sometimes, with implicit inclusion of the effect of the medium) rather than crystals, are much more user friendly. However, in most cases this excludes the possibility of the first-principle calculations of substances in the condensed state and materials based on them.

Another reason consists in high system requirements that should be met to provide stable operation of software. Generally, such labour-consuming calculations require a computer cluster or a multiprocessor system with a large amount of random access memory and disc storage rather

A A Korlyukov, M Yu Antipin A N Nesmeyanov Institute of Organoelement Compounds, Russian Academy of Sciences, ul. Vavilova 28, 119991 Moscow, Russian Federation. Fax (7-499) 135 50 85, tel. (7-499) 135 92 14, e-mail: alex@xrlab.ineos.ac.ru (A A Korlyukov). tel. (7-499) 135 92 15, e-mail: m_antipin@yahoo.com (M Yu Antipin)

Received 3 February 2011
Uspekhi Khimii **81** (2) 105 – 129 (2012); translated by A M Raevskiy

than a personal computer as in the studies of isolated molecules. However, with the development of computer hardware (in particular, better accessibility of supercomputers) the problem becomes less complicated. Modern quantum chemical calculations of crystals can provide information that is hard to obtain in theoretical studies of isolated molecules or small molecular aggregates.

In this review we briefly outline the density functional theory and methods of calculations of crystal structures. The potential of DFT quantum chemical calculations with periodic boundary conditions will be illustrated by relevant examples and appropriate software will be characterized. Examples are taken from publications reported during the last decade and from our own studies. Crucial importance of quantum chemical calculations of structural parameters in studies of polymorphism will be shown.

II. DFT functionals, basis sets and pseudopotentials

The development of the density functional theory is related to the Hohenberg–Kohn theorems from which, in particular, it follows that all properties of a system are completely determined by the density distributions (ρ) for the constituent particles. Based on this fact, Kohn and Sham assumed that the ρ value for the ground state of a system of interacting particles (*e.g.*, atomic nuclei and electrons) is equal to that for a system of noninteracting particles chosen in some way.

The ground-state energy of a system of noninteracting atomic nuclei and electrons (E_{KS}) is a functional of ρ. It is defined as follows:

$$E_{KS}[\rho] = T[\rho] + \int d\boldsymbol{r} V_{ext}(\boldsymbol{r})\rho(\boldsymbol{r}) + E_H[\rho] + E_{nn} + E_{xc}[\rho], \quad (1)$$

where T is the kinetic energy of the system of noninteracting atomic nuclei and electrons

$$T = \frac{1}{2}\sum_{\sigma}\sum_{i=1}^{N^{\sigma}}|\psi_i^{\sigma}|^2, \quad (2)$$

ψ_i^{σ} are the one-electron wave eigenfunctions (index σ indicates the spin dependence of a particular value); V_{ext} is the external potential independent of electron spins (*e.g.*, external electric field or hydrostatic pressure); $\rho(\boldsymbol{r})$ is the electron density of the system of N ($N = N\uparrow + N\downarrow$) electrons with N^{σ} orbitals ψ_i^{σ} (symbols $\uparrow$ and $\downarrow$ denote the directions of electron spin),

$$\rho(\boldsymbol{r}) = \sum_{\sigma}\rho(\boldsymbol{r},\sigma) = \sum_{\sigma}\sum_{i=1}^{N^{\sigma}}|\psi_i^{\sigma}|^2; \quad (3)$$

E_H is the Coulomb energy characterizing the self-interaction property of the electron density

$$E_H[\rho] = \frac{1}{2}\int d\boldsymbol{r}d\boldsymbol{r}'\frac{\rho(\boldsymbol{r})\rho(\boldsymbol{r}')}{|\boldsymbol{r}-\boldsymbol{r}'|}, \quad (4)$$

$\boldsymbol{r}$ and $\boldsymbol{r}'$ are the generalized coordinates, E_{nn} is the energy of the interaction between atomic nuclei, and E_{xc} is the exchange-correlation energy. The notation $[\rho]$ means that the value is a functional of the electron density and depends on the spin σ and generalized coordinate $\boldsymbol{r}$.

Knowing the form of the functional $E_{xc}[\rho]$, the ground-state energy can be calculated using the Kohn–Sham equation

$$(H_{KS}^{\sigma} - e_i^{\sigma})c_i^{\sigma} = 0, \quad (5)$$

H_{KS}^{σ} is the Hamiltonian of the system and ε_i^{σ} are the eigenvalues of the Hamiltonian;

$$H_{KS}^{\sigma} = -\frac{1}{2}\nabla^2 + V_{KS}^{\sigma}(\boldsymbol{r}). \quad (6)$$

Here ∇^2 is the Laplace operator, V_{KS}^{σ} is the potential of the ground state of the system of interacting electrons

$$V_{KS}^{\sigma}(\boldsymbol{r}) = V_{ext}(\boldsymbol{r}) + V_H(\boldsymbol{r}) + V_{xc}^{\sigma}(\boldsymbol{r}), \quad (7)$$

where $V_H(\boldsymbol{r})$ is the Hartree potential and $V_{xc}^{\sigma}(\boldsymbol{r})$ is the exchange-correlation potential.

The Kohn–Sham equations are analogues of the one-electron equations in the Hartree–Fock method. The potential, energy of the system and the electronic energy can be calculated using the self-consistency procedure.

According to Kohn and Sham, the exchange-correlation energy can be defined as the integral of the one-electron exchange-correlation energy (*i.e.*, the energy per electron at the point r; it depends only on the electron density in the vicinity of the point r)

$$E_{xc}[\rho] = \int d\boldsymbol{r}\rho(\boldsymbol{r})\varepsilon_{xc}([\rho],\boldsymbol{r}). \quad (8)$$

Exact analytical form of the expression for E_{xc} is unknown. According to the local spin density approximation (LSDA), is it assumed that the value E_{xc}^{LSDA} is equal to the corresponding value for a homogeneous electron gas at any point of the system

$$E_{xc}^{LSDA}[\rho\uparrow,\rho\downarrow] = \quad (9)$$
$$= \int d\boldsymbol{r}\rho(\boldsymbol{r})[\varepsilon_x^{hom}(\rho\uparrow(\boldsymbol{r}),\rho\downarrow(\boldsymbol{r}) + \varepsilon_c^{hom}(\rho\uparrow(\boldsymbol{r}),\rho\downarrow(\boldsymbol{r})],$$

where ε_x^{hom} and ε_c^{hom} are the one-electron exchange energy and the correlation energy of homogeneous electron gas, respectively.

For a system with all electrons paired (local density approximation, LDA), one has

$$\rho(\boldsymbol{r})\uparrow = \rho(\boldsymbol{r})\downarrow = \frac{\rho(\boldsymbol{r})}{2},$$

and the number of equations is halved.

Various analytical expressions for the one-electron exchange energy of homogeneous electron gas are available. The one-electron correlation energy can be calculated numerically. Different analytical expressions to approximate ε_x^{hom} were proposed by Perdew and Zunger,[3] Vosko, Wilks and Nusair,[4] and also by Lee, Yang and Parr.[5] The LDA approximation quite correctly describes crystals in which electrons can be treated as electron gas (*e.g.*, crystals of some metals), but works poorer for systems with localized bound electrons.

This drawback of the LDA gave an impetus to the development of the generalized gradient approximation (GGA). The quantity ε_x^{hom} in the expression for the exchange-correlation energy determined by the GGA method is treated as a functional of not only the electron density $\rho^\sigma(\boldsymbol{r})$, but also its gradient $\nabla\rho^\sigma(\boldsymbol{r})$,

$$E_{xc}^{GGA} = \int d\boldsymbol{r}\rho(\boldsymbol{r})\varepsilon_x^{hom}(\rho)F_{xc}(\rho\uparrow, \rho\downarrow, |\nabla\rho\uparrow|, |\nabla\rho\downarrow|, ...). \quad (10)$$

Numerous expressions (functionals) were proposed for the correction function F_{xc}. Most quantum chemical calculations of molecular crystals use the functionals BP or BP88,[6,7] BLYP, PW91,[8] PBE,[9] and its modified version, RPBE functional.

Description of the electron density as functional of not only $\nabla\rho^\sigma(\boldsymbol{r})$, but also the Laplacian $\nabla^2\rho^\sigma(\boldsymbol{r})$ and the kinetic energy density allows one to formulate the meta-GGA approximation. Compared to conventional GGA functionals, the meta-GGA functionals are not so often used in quantum chemical calculations. Most often, programmes for calculations of crystals use PKZB,[10] a modified PBE functional.

Better results are obtained using the so-called hybrid functionals which in essence represent combinations of the exchange contributions determined by the Hartree–Fock method and using DFT functionals. An example is provided by the PBE0 hybrid functional[9] which includes a 25% contribution of the Hartree–Fock (HF) exchange energy (E_x^{HF}),

$$E_{xc} = E_{xc}^{LDA} + \frac{1}{4}(E_x^{HF} - E_{xc}^{PBE}), \quad (11)$$

where the superscript (LDA, HF and PBE) denotes the method of calculations of the exchange-correlation energy. The contribution E_x^{HF} is an empirical parameter.

Yet another hybrid functional incorporated into most quantum chemical programmes for studies of crystals is B3LYP[11] containing three empirical parameters. The expressions for E_{xc} in the most widely known DFT functionals can be found not only in the original studies, but also in Refs 12 and 13.

The GGA and meta-GGA functionals allow one to successfully calculate the interatomic distances and force constants for the ground state of most diatomic molecules, the unit cell parameters and elastic moduli of many binary compounds (oxides, carbides, nitrides). However, the forbidden gaps in semiconductors and conductors are often calculated incorrectly. The choice of the GGA and meta-GGA functionals to study excited states is also inappropriate.

The results of quantum chemical calculations of the band gaps using hybrid functionals much better agree with experimental data, but they are more time-consuming compared to the calculations using the GGA and meta-GGA functionals.

To solve the Kohn–Sham equations, one should have a finite basis set that is large enough to describe the wave function. Isolated molecules are often studied using basis sets composed of localized atom-centred functions. This type of functions can be either analytical or numerical. When using analytical functions (as a rule, Gaussian ones), all matrix elements can be expressed analytically. In essence, the Gaussian functions are eigenfunctions of the harmonic oscillator and, therefore, they can be obtained by solving the Schrödinger equation. But they are inconvenient in use because their form differs from that of the radial functions obtained in the solution of the Schrödinger equation for hydrogen-like atoms (atomic orbitals). Therefore, Gaussian functions are usually transformed to a more convenient form used in solving quantum chemical problems. Combining some Gaussian functions with fixed coefficients a makes it possible to construct some functions called Gaussian-type orbitals (GTO) or Slater-type orbitals (STO):

$$R(\boldsymbol{r}) = a\,e^{-ar^2}, \quad (12)$$

$$R(\boldsymbol{r}) = a\,e^{-ar}. \quad (13)$$

As a rule, it is functions (12) and (13) that are used as basis sets. Examples of the basis sets constructed from Gaussian functions (usually called 'primitive Gaussian functions') are provided by the $X-YZG$, $X-YZWG$ and $X-YZWVG$ Pople basis sets.[14,15] Atomic orbitals corresponding to core electrons are constructed using X (usually, from 3 to 8) primitive basis functions. Atomic orbitals of valence electrons are constructed using Gaussian functions with different coefficients and pre-exponents. The number of types of these functions varies from two (YZ) to four ($YZWV$). The basis set can be augmented with some functions to improve the description of regions distant from atomic nuclei (diffuse functions) or with functions that describe the electron density redistribution as a result of formation of a molecule or a crystal (polarization functions). It should be noted that the diffuse functions are almost not used in studies of crystals because in this case the computational cost significantly increases and the calculations become much slower (see, *e.g.*, a User's guide to the CRYSTAL programme†). The Pople basis sets have a very flexible structure and allow one to solve various tasks with moderate computational cost.

The STO basis sets are much less convenient, especially in studies of crystals because a larger number of primitive Gaussian functions is required for constructing a basis set of reasonable accuracy. Consequently, the computational cost increases. Fortunately, the STO functions can be obtained using the results of high-precision quantum calculations of isolated atoms (as is implemented in the ADF/BAND programme;[16] in this case, the basis set will be much smaller than the Pople basis sets.[14] A similar procedure is used to obtain the radial functions (so-called pseudoatomic orbitals) which are then employed to construct the basis sets (numerical STO NZ basis sets with $N = 2, 3$). A drawback of the GTO and STO basis sets (*i.e.*, localized basis sets) is systematic overestimation of the energy of loosely bound systems (including molecular crystals) owing to the so-called basis set superposition error (BSSE), *viz.*, difference between the basis sets for the entire system and for each individual molecule. The value of this error depends on the size of the basis set. Usually, the account of BSSE is made by the counterpoise method; calculations are carried out for each molecule in the system using the basis set for the entire system and assuming zero atomic charges on other molecules in the system.

† http://www.crystal.unito.it/Manuals/crystal09.pdf

Plane waves represent another type of analytical functions which can be used only in calculations with periodic boundary conditions. This type of basis set was for the first time proposed by Slater [17] (method of augmented plane waves); numerous theoretical approaches based on his ideas have been reported to date.[12, 13] In performing quantum chemical calculations of crystals one should take into account their three-dimensional long-range order using periodic boundary conditions. Any periodic wave function can be expanded into a Fourier series. A one-electron wave function can be represented by the sum of plane waves

$$\psi_i(\boldsymbol{r}) = \sum c_{i,G} \frac{1}{\sqrt{V}} e^{iG\boldsymbol{r}}, \quad (14)$$

where $c_{i,G}$ are the expansion coefficients, V is the unit cell volume and G is the reciprocal lattice vector.

Thus, plane waves form a complete orthonormalized basis set used to solve the Kohn–Sham equations. Plane waves are not centred on atomic nuclei and the accuracy of the description of a wave function using this type of basis set will be the same at any point of the system. The advantage of the plane wave approach is the lack of BSSE. By increasing the number of plane waves in the basis set one can improve the accuracy of calculations. However, in practice the basis set for calculations is specified by the kinetic energy cutoff rather than the number of plane waves. Taking account of atomic core electrons whose wave functions are characterized by oscillations in the vicinity of a nucleus requires a very large number of plane waves in the expansion over the basis set functions. Therefore, the core electrons are described using pseudopotentials. Usually, pseudopotentials are derived based on the results of solution of the Schrödinger equation or relativistic Dirac equation for isolated atoms. In the latter case, the relativistic effects for core electrons (usually, spin–orbit interaction) are taken into account.

Quantum chemical calculations are carried out using pseudopotentials with norm conservation (local pseudopotentials) as well as pseudopotentials without norm conservation (nonlocal or ultrasoft-pseudopotentials [18] or the projected augmented wave technique [19, 20]). An analysis of published data showed that for the first type of pseudopotentials the maximum kinetic energy is at least 900 eV. Of course, this holds only for molecular crystals of organic and organoelement compounds. Nonlocal pseudopotentials do not require such a large basis set (the maximum kinetic energy varies from 300 to 600 eV). This is attained by augmentation with functions localized on the atomic nucleus, or the so-called compensation charges. The wave-function component corresponding to the pseudopotential (pseudowave function) should be continuous and differentiable. At distances longer than the radius of the pseudopotential (R_c), the pseudowave function matches the full-electron wave function to an accuracy of the normalizing factor. To take into account core electrons, some local pseudopotentials are augmented with a constant contribution of the charge density in the vicinity of the atomic nucleus (partial core correction). Unfortunately, in many cases this causes the second derivative of the wave function to undergo discontinuity in the vicinity of R_c;[12] this makes such pseudopotentials inappropriate for calculations of many properties. Nonlocal pseudopotentials are free from this drawback. General types of local and nonlocal pseudopotentials, as well as mathematical formalism used to describe them are available from monographs. [12, 21]

It should be noted that a basis set including localized functions can also be used with pseudopotentials. This makes it possible to reduce the computational cost and take account of relativistic effects, which is particularly important in the case of atoms of heavy elements (starting from period IV elements), for which the development of high-precision, small basis set is a serious problem .

III. The software: a brief survey

A large array of software for quantum chemical calculations of crystals has been developed but consideration of all programmes is senseless because most of them represent open-code software written and supported by particular research groups or enthusiasts. Nevertheless, there is also commercially available software which can cost from a few hundreds to a few tens of thousands US dollars (or euro). However, the price does not indicate the quality or versatility of functional possibilities because a high price is often due to technical support or unique algorithms for solution of complicated tasks.

The available software can conditionally be divided into two groups depending on the basis set employed. The first group includes programmes that use various types of localized basis sets implemented in them while the second group includes programmes with the plane wave basis set. The first type of programmes is simpler in use for chemists because the basis set used in them is much like that employed in the popular programmes GAMESS-US (see Ref. 22) or Gaussian.[23]

Programmes that use the plane wave basis set do not explicitly include the effects of core electrons; nevertheless, they can be used to, *e.g.*, calculate the chemical shifts in the NMR spectra of crystals.

There is considerable literature devoted to comparison of the programmes that use different types of basis sets (see, *e.g.*, Refs 24–29) but these studies revealed no decided advantages of a particular type of basis set over other basis sets. The results to a great extent depend on the efforts made by the software development teams, namely, on the timely incorporation of implementations of the newest theoretical methods into programmes in order to overcome the drawbacks of the LCAO-MO or plane wave approximations. Programmes using both mixed plane wave basis sets and Gaussian functions, *e.g.*, CP2K,[26] Quickstep,[30] and Wien2k [31] are also available. However, these programmes were in fact used only in the study of inorganic compounds, semiconductors and metals.

The characteristics of the most widely used software for calculations of crystals are summarized in Table 1. The programmes presented in Table 1 demonstrate a conventional set of features including optimization of atomic coordinates and unit cell vectors, calculations of vibrational spectra, and energy band structure calculations. Also, algorithms incorporated into these programmes (except CRYSTAL) allow one to carry out the molecular dynamics calculations.

The list of programmes (see Table 1) is far from being complete, but it does include the programmes that are most widely used in studies of molecular crystals by computational methods.

Table 1. Characteristics of software used for calculations of crystals of organic and organoelement compounds.

Software name	Distribution conditions	Basis set (type of pseudopotential)	DFT methods	Specific features	Ref.
CASTEP (see [a])	see [b]	PW (USPP, TM)	L(S)DA, GGA	NMR, EPR	33
Dmol3 (see [a])	no separate distribution	numerical *NZ*-basis set (TM)	L(S)DA, GGA		34
VASP	Euro 3000/licence	PW (PAW)	L(S)DA, GGA meta-GGA, hybrid, MP2	taking account of the van der Waals correction, NMR	35 – 37
CPMD	free	PW (TM, USPP)	L(S)DA, GGA	taking account of the van der Waals correction, NMR, EPR	38
CRYSTAL	USD 900/licence	GTO	L(S)DA, GGA meta-GGA, hybrid, MP2 [c]	taking account of the van der Waals correction	39
Quantum ESPRESSO	free	PW (USPP, TM, PAW)	L(S)DA, GGA	taking account of the van der Waals correction, NMR, EPR	40
SIESTA		PW (TM)	L(S)DA, GGA		41

Note. Notations are as follows: 'NMR' and 'EPR' denote calculations of NMR and EPR spectroscopic parameters, 'hybrid' denotes hybrid functionals, 'PW' stands for plane waves, 'USPP' stands for Vanderbilt ultrasoft pseudopotentials,[18] 'TM' stands for Troullier – Martins pseudopotentials,[32] and 'PAW' stands for the Projector Augmented Wave method.[19, 20]

[a] Part of the Material Studio software environment. [b] Free separate distribution only for academic institutions at the United Kingdom. [c] The method is implemented in a particular version of the programme which is provided at extra charge.

IV. The accuracy of calculations, reproduction of unit cell parameters and taking account of the van der Waals correction

A main problem in DFT is related to difficulties in taking account of the effect of weak (but, usually, multicentre) interatomic interactions. In the case of molecular crystals, this leads to significant differences between the calculated and experimental values of interatomic distances that characterize intermolecular interactions. As a consequence, the optimized (calculated) and experimental values of the unit cell parameters of crystals, as well as their enthalpies of sublimation differ appreciably.

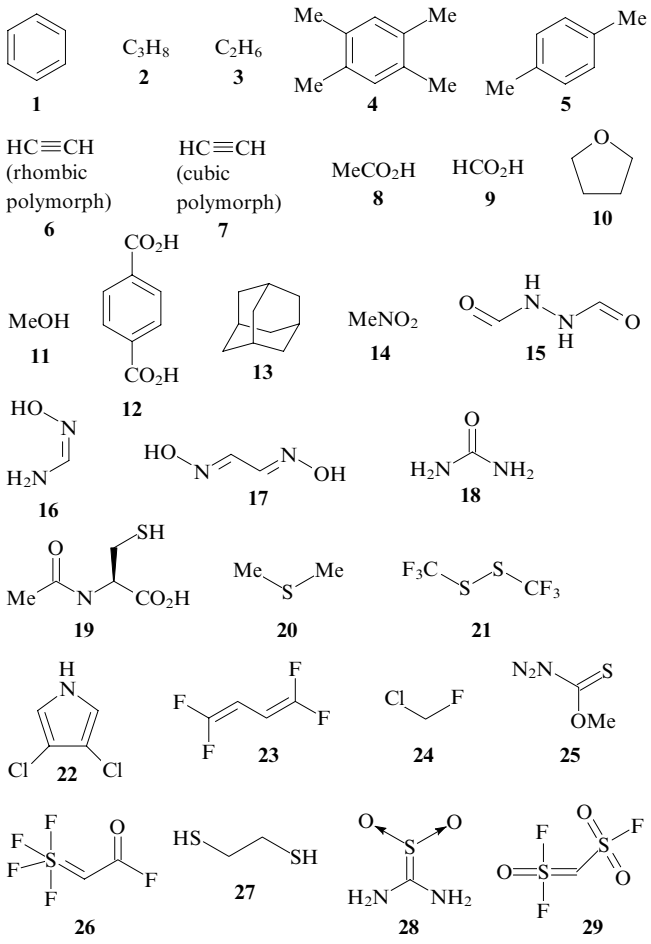
An example is provided by the PW91 exchange-correlation functional (plane wave basis set). In this case, the average relative deviation (ΔV) of the calculated (V_1) unit cell volume from the experimentally determined value (V_2)

$$\Delta V = \frac{V_1 - V_2}{V_1}$$

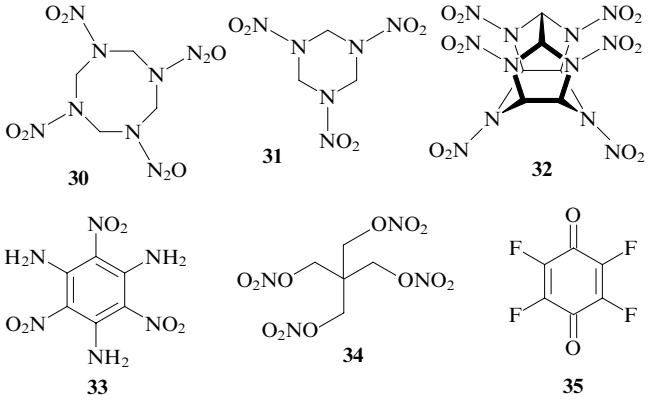
appears to be 20% for a set including 29 structures of simple organic substances **1** – **29**.[42]

It was found that the unit cell volume is systematically overestimated. This is probably an indication of errors in the description of mutual attraction of molecules in the crystal. The root-mean-square deviation of the calculated atomic coordinates relative to the experimental values is 0.045 Å. Errors obtained in calculations of the interatomic distances in the crystals of nitromethane and some other energetic materials using the PW91 functional[43] are of nearly the same order of magnitude (0.037 Å for nitromethane). An increase of the kinetic energy cutoff from 330 to 700 eV did not improve the agreement between calculated and experimental data.

Modelling the effects of hydrostatic pressure on the structure of energetic materials, such as HMX (**30**), hexogen (**31**), hexanitrohexaazaisowurtzitane (**32**), triaminotrinitrobenzene (**33**) and pentaerythritol tetranitrate (**34**) using the PW91 and PBE functionals revealed systematic overestima-



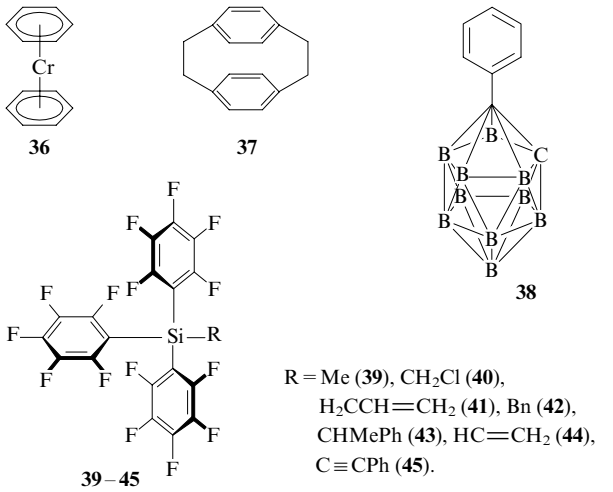
tion of the unit cell volume at pressures below 5 GPa.[44] Further increase in pressure (to 10 GPa) led to better agreement between the results of calculations and experimental data. Such a 'behaviour' of the PW91 functional seems to be an indication of a common trend. For instance, consider the case for tetrafluoro-*p*-benzoquinone (**35**).[45] In the crystal of compound **35**, an important role is played by stacking interactions as well as H···F and F···F interactions. Here, the calculated value of the unit cell volume remains larger than the experimental value at 120 K even as the pressure increases to 4 GPa. For comparison, MP2/6-31 + + G(d,p) calculations[46] of the α-phase of solid methanol (atomic packing was modelled by a cluster) gave good agreement with experimental data. The calculated unit cell volume appeared to be only 2.5% smaller than the experimental value.



30 **31** **32** **33** **34** **35**

Thus, the aforesaid suggests that overestimation of the unit cell volume and, correspondingly, underestimation of attractive intermolecular forces do not allow DFT (at least the widespread PW91 and PBE functionals) to be used for prediction of parameters of crystals (first of all, their densities). However, this is not an unambiguous statement. For instance, in the complexes of arenes with perfluoroarenes, electrostatic attraction through stacking interaction and interactions involving fluorine atoms makes a more than 90% contribution to the cohesive energy (sublimation energy).[47,48] In spite of the differences between the calculated and experimental values of the unit cell volume, the interatomic distances characteristic of intermolecular interactions were determined with an acceptable accuracy (PW91/400 eV, calculations with the plane wave basis set).

Examples of good agreement between the values obtained by extrapolating experimental data to 0 K and the calculated data on the cohesive energy at 0 K are provided by the data for dibenzenechromium(III) (**36**)[49] (PBE/408 eV) and [2,2′]-paracyclophane (**37**)[50] (HCTH/120/300 eV) crystals. The calculated energies are 22.9 and 16.0 kcal mol^{-1} [*cf.* experimental values of 23.0 ± 1.0 (Refs 51 and 52) and 18.7 kcal mol^{-1} (Ref. 53), respectively]. The experimental value of the sublimation energy for the crystal of 1-phenyl-*o*-carborane (**38**)[54] is unknown, but the results of its evaluation based on the results of topological analysis of experimental electron density distribution function and quantum chemical calculations (PBE/340 eV) agree well with each other (17.0 and 16.4 kcal mol^{-1}, respectively).

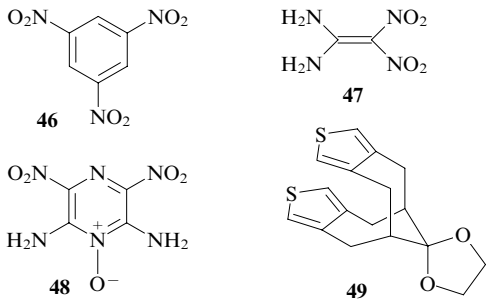


36 **37** **38** **39–45**

R = Me (**39**), CH_2Cl (**40**), $H_2CCH{=}CH_2$ (**41**), Bn (**42**), CHMePh (**43**), $HC{=}CH_2$ (**44**), C≡CPh (**45**).

A study[55] (LDA/300 eV) of a series of structurally similar crystals of tris(pentafluorophenyl)silanes **39**–**45** revealed a correlation between the sublimation energy and the melting point. This result is interesting because, generally, such a correlation is not necessary and can be observed only for groups of related compounds (*e.g.* , for homologues). To estimate the calculated cohesive energies of compounds **36**–**45**, the authors of Ref. 55 compared the results obtained using different functionals and reported only the results of those calculations that gave the molecular geometry (atomic coordinates) and cohesive energy values consistent with the experimental data.

The sublimation energy values of polynitro compounds **30**–**33**, 2,4,6-trinitrotoluene (**46**), 2,2-dinitroethene-1,1-diamine (**47**), 2,6-diamino-3,5-dinitropyrazine 1-oxide (**48**) and benzene derivatives obtained from PBE/DNP‡ calculations[56] differ from the corresponding experimental data. Usually, the differences were at most 1.2 kcal mol^{-1}, but for compounds **33** and **46** they appeared to be 4.6 and −6.2 kcal mol^{-1}, respectively. The large differences seem to be due to specific features of the unusual approach used in Ref. 56. Calculations were carried out using a simple cubic cell with the parameter $a = 25$ Å rather than the experimental lattice constants and space group. During the optimization procedure, positions of molecules could be significantly changed owing to the lack of symmetry restrictions, which eventually led to differences between the sublimation energy values.



46 **47** **48** **49**

When using the plane wave basis set, there is no need to take into account the BSSE; however, this is not the case if a localized basis set is employed. In particular, for a crystal of

‡ The exact name is the Double Numerical plus Polarization (DNP) basis set.

urea (**18**) the inclusion of BSSE leads to systematic underestimation of the enthalpy of sublimation. Calculations with the hybrid functional B3LYP underestimate the enthalpy of sublimation of urea crystal by 7.2 kcal mol^{-1} irrespective of the basis set.[57]

Difficulties in the reproduction of the experimental values can be overcome using the 'post-Hartree-Fock' methods with inclusion of electron correlation (*e.g.*, the MP2 method); however, the computational cost appears to be too high. Some software development teams prefer to improve the DFT functionals. Considering software for calculations of crystals, mention may be made of the PBEsol[58] (reparameterization of PBE) and AM05[59] functionals, which give better agreement between the results of calculations and experimental data compared to the PBE or PW91 functionals, even in the description of chemical reactions.[60] Unfortunately, the results of quantum chemical calculations of crystals of organic or organoelement compounds with these functionals were reported only for one compound **49**.[61] Note that in this case, the PBEsol functional was used in combination with the van der Waals correction (see below).

Another strategy involves combining DFT and the force field theory which describes long-range forces; in essence, this means introducing empirical corrections. A drawback of this approach consists in the need for calculating parameters of pair interactions between all types of atoms in the crystal. Schemes of calculations of such parameters and the results obtained are available in the literature (see, *e.g.*, Refs 42 and 62–65). A detailed description of this approach taking calculations of isolated molecules and molecular associates as examples can be found in a review by Hobza and co-workers.[66] Most programmes include a scheme developed by Grimme.[63] Within the framework of the Grimme scheme, the total energy of a crystal is given by

$$E_{\mathrm{DFT}} = E_{\mathrm{KS}} + E_{\mathrm{disp}} ,$$

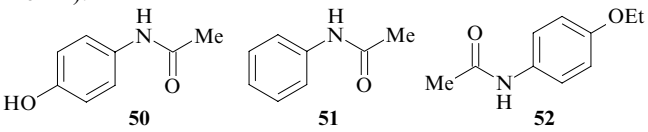
where E_{KS} and E_{disp} are the contributions due to solution of the Kohn–Sham equations and taking into account the dispersion correction, respectively. The last term in the expression can be calculated as the sum of pair empirical potentials for any number of atoms N

$$E_{\mathrm{disp}} = -s_6 \sum_{i=1}^{N-1} \sum_{j=i+1}^{N} \frac{C_6^{ij}}{R_{ij}^6} f_{\mathrm{dmp}}(R_{ij}) , \qquad (15)$$

where s_6 is the scale factor depending on the type of the functional, C_6^{ij} are empirical coefficients determined from the London relation, R_{ij} is the interatomic distance; and the damping function $f_{\mathrm{dmp}}(R_{ij})$ is used to avoid singularities in the vicinity of atoms.

Corrections introduced into the scheme of quantum chemical calculations are called the van der Waals and dispersion corrections. Taking account of these corrections for compounds **1**–**29** (see above) leads to a decrease in ΔV values down to 1% on the average. A maximum ΔV value equal to 3.2% was obtained for crystal **11**.

The van der Waals correction introduced into calculations of crystal **14** led to a small (0.7%) increase in the unit cell volume, whereas calculations without this correction overestimated the unit cell volume by 12% (PW91/700 eV).[67] The introduction of empirical corrections made it possible to reproduce the enthalpy of sublimation of paracetamol (**50**) and acetanilide (**51**).[68] Indeed, the calculated values are 28.9 (**50**) and 23.7 (**51**) kcal mol^{-1} (*cf.* experimental values of 28.1 ± 0.2 and 23.8 ± 0.2 kcal mol^{-1}, respectively). The difference obtained for phenacetin (**52**) is 0.5 kcal mol^{-1}. This value is somewhat larger than for compounds **50** and **51** but lies within the limits of measurement error (experimental value is 27.6 ± 0.6 kcal mol^{-1}).[69]

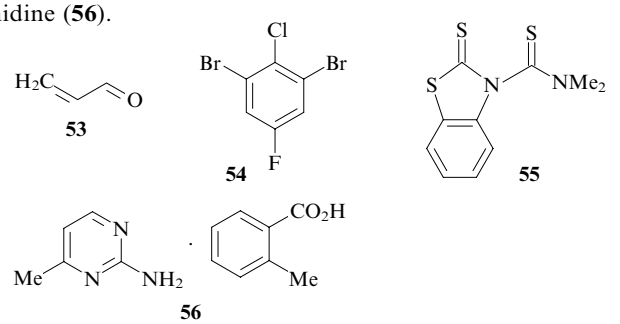


Advances in reproduction of energy characteristics and unit cell parameters of crystals using empirical corrections suggest the possibility of analyzing rather subtle effects, such as stabilization of eclipsed or staggered conformation of methyl groups in methyllithium tetramers.[70] It is crucially important that this type of calculations offers prospects for carrying out stability analysis of different polymorphs and searching an answer to the question what is the contribution of the thermodynamic factor to crystalization of particular polymorphs. These studies are of great importance for research on polymorphism of pharmaceuticals (see below).

V. Studies of the relative stability of polymorphs

In this Section, we will consider issues concerning quantum chemical calculations of structural parameters and comparison of the energies of polymorphs, which are of importance for solution of industrial problems, especially problems in pharmaceutical industry. Sometimes, crystallization leads to formation of mixed crystals (co-crystals) and crystal solvates (pseudopolymorphs). Stability prediction of such crystalline polymorphs can be useful for the development of optimal process conditions for industry. Therefore, rapid progress in crystal chemistry studies of the polymorphism and structure of co-crystals by computational methods (usually, by empirical and semiempirical ones)[71,72] is not surprising.

If the structures of some polymorphs are unknown or a test procedure is developed, the atomic coordinates can be generated using the site–site potentials and relevant software.[73–75] Further optimization of structures can be done by quantum chemistry methods. A very interesting study[76] is devoted to *ab initio* prediction ('blind' test) of the crystal structures of three organic compounds (**53**–**55**) and a co-crystal of 2-methylbenzoic acid and 2-amino-4-methylpyrimidine (**56**).



The initial approximations were obtained using the site–site potentials and then the search for crystal structures was carried out. Calculations with a multiprocessor

system (48 CPUs) took 4 months. A set of structures with very close energies was generated; it included the experimentally studied systems. Difficulties in prediction of the thermodynamic stability of the polymorphs of conformationally flexible molecules are due to small energy differences between them. Then, the results obtained were used in DFT calculations with inclusion of van der Waals corrections. This allowed rejecting the energetically unfavourable structures and thus reducing the number of the structures under consideration. Eventually, three possible polymorphs were chosen for each structure; the energy differences between the polymorphs were at most 0.059 kcal mol^{-1} atom^{-1}. The experimental structures appeared to be the most energetically favourable. This makes it possible to use DFT calculations for comparing the thermodynamic stabilities of polymorphs.

Yet another study[77] of polymorphism concerned acetic acid polymorphs (BP/952 eV, with van der Waals correction). Only the orthorhombic polymorph can be grown under standard conditions;[78] the monoclinic polymorph was obtained at a pressure of 0.2 GPa (Fig. 1).[79] The structure of this compound shows no dimerization through O—H···O bonds both under standard conditions and at elevated pressure. These bonds link molecules to form chains. Indeed, the energies of all generated structures for which dimerization is possible, are 0.2–5.5 kcal mol^{-1} higher than the energies of the experimental structures. Numerical values of the van der Waals correction were nearly equal for all polymorphs studied (12.7–13.5 kcal mol^{-1}).[77] These corrections should be taken into account in order to reproduce experimental unit cell parameters and to obtain the most realistic interatomic distances. Moreover, it was assumed[76] that the predictive power of quantum chemical calculations can be improved by taking account of zero-point vibrational enegy correction and the entropy contribution, which are usually ignored.

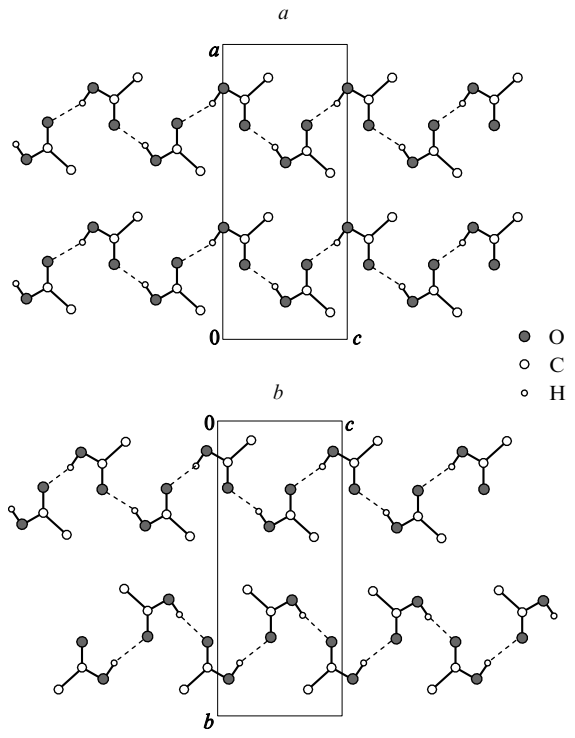


Figure 1. Chains formed through O—H···O bonds in the orthorhombic (*a*) and monoclinic (*b*) polymorphs of acetic acid.

At the same time, the introduction of all corrections into the scheme of DFT calculations is a labour- and time-consuming procedure (fortunately, tabulated sets of parameters are available for many programmes). Therefore, it is of interest to establish whether one can reliably characterize polymorphs using conventional (unmodified) functionals. Now we will briefly outline some examples.

The energy difference between the monoclinic and tetragonal polymorphs of trimethylborane BMe_3 (PW91/540 eV) is 0.4 kcal mol^{-1} (Ref. 80). Indirect data[80] suggest a lower stability of the tetragonal polymorph.

The amount of information on different polymorphs of glycine (**57**) is much larger. Probably, this gave an impetus to a number of thorough studies of this compound, which is often considered as a model (test) system for various calculations. Quantum chemical calculations of the α-, β- and γ-polymorphs of glycine (Fig. 2) were carried out using the plane wave basis set (PW91, PBE and LDA functionals, 450 eV)[81] and the doubly split, localized DNP basis set (BLYP functional).[82] According to BLYP/DNP calculations, the energy of the α-polymorph of glycine is 0.55 and 0.48 kcal mol^{-1} lower than those of the β- and γ-polymorphs, respectively. The root-mean-square deviation of the calculated atomic coordinates from experimental ones was 0.21 Å, which is due to differences in the location of hydrogen atoms (their positions are determined with insufficient accuracy by X-ray diffraction analysis). Calculations by the LDA method and the plane wave basis set give a smaller value of the unit cell volume (by 7%–12%); however, they correctly reproduce the order of the relative stabilities of the polymorphs (γ-polymorph is 0.3 and 0.6 kcal mol^{-1} more stable than the α- and β-polymorphs, respectively). Calculations using the PBE and PW91 functionals give somewhat larger unit cell volume and predict that the energy of the α-polymorph is 0.2–0.3 kcal mol^{-1} lower. A stability study[83] of the α- and γ-polymorphs of glycine with the DNP basis set and a very large number of functionals showed the importance of taking into account the zero-point vibrational energy correction and the vibrational contribution to the enthalpy (*i.e.*, corrections for the temperature dependence of vibrational energy in the crystal). Quantum chemical calculations using the BLYP, BOB and RPBE functionals carried out ignoring these corrections showed that the α-polymorph is more stable than the γ-polymorph (energy difference is 0.06–0.12 kcal mol^{-1}). Contrary to this, calculations with other functionals (BP, PBE, PW91, VWNBP) showed the energy preferableness of the γ-polymorph. Taking account of zero-point vibrational energy correction and vibrational contribution to the enthalpy led to correct reproduction of the relative stability order of the α- and γ-polymorphs of compound **57** for all functionals. The energy difference was in the range from 0.12 to 0.24 kcal mol^{-1}; the minimum and maximum values were obtained for the BP and PBE functionals, respectively (experimental value is 0.06 kcal mol^{-1}).[83]

Analogously, B3LYP/6-311G(d) calculations using the hybrid functional with inclusion of corrections for zero-point vibrational energy and the entropy contribution allowed the energy difference between the polymorphs of *N*,*N*′-dimethylurea to increase from 0.05 to 0.1 kcal mol^{-1} (Ref. 84).

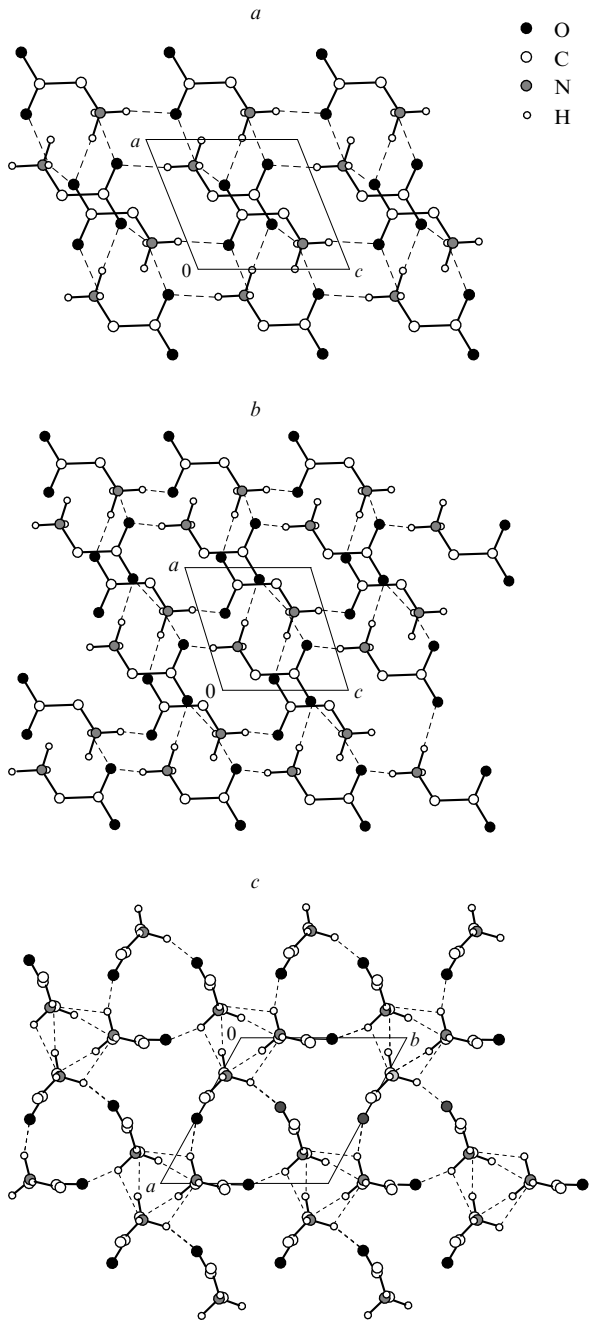


Figure 2. General view of crystal packings of the α- (*a*), β- (*b*) and γ-polymorphs (*c*) of glycine: projections on the *ac*, *ac* and *ab* plane, respectively.[81,82]

Stability prediction of the polymorphs of *p*-diiodobenzene (**58**) within the framework of the DFT appeared to be a complicated task.[85] According to experimental data,[86] β-polymorph is more stable than the α-polymorph (energy difference between them is 2.21 kcal mol^{-1}). Among conventional functionals, only LDA correctly reproduced the relative energies of the polymorphs, which were overestimated by 0.63 kcal mol^{-1} compared to the experimental stability of the β-polymorph. Calculations with the PW91 and PBE functionals showed that the α-polymorph is the most stable, although the energy difference was small (0.67 and 0.58 kcal mol^{-1}, respectively). The hybrid functional B3LYP led to even larger energy difference (1.57 kcal mol^{-1} in favour of the α-polymorph). Only when the van der Waals correction to the B3LYP functional was applied, the relative stabilities of the polymorphs of compounds **58** appeared to be estimated correctly; however, the β-polymorph was overestimated by 1.36 kcal mol^{-1} compared to experimental data. The best result was obtained using quantum chemical Monte Carlo calculations, but in this case the standard deviation was very large; this was associated[85] with too small chain length in the calculations (owing to specific features of the computational method).

Thus, when the van der Waals correction is ignored, reproduction of the thermodynamic properties of polymorphs depends strongly on the functional chosen; note that criteria for the choice of the functional are ambiguous. Hybrid functionals seem to be inefficient because the computing time increases. Apparently, the choice of a functional requires test calculations of model crystals.

Polymer crystals represent more complex systems for studies of polymorphism because data on their structures are scarce. As an example, one can consider polymorphism of poly(lactic acid) having three experimentally detected polymorphs (α, β and γ). Three structural types were proposed for the α-form (space groups $P\bar{1}$ and $P2_12_12_1$); the other two forms crystallize in the groups $P3_2$ (β) and $P2_1$ (γ). All these forms were studied using the PW91 functional and the plane wave basis sets (340 eV) and DNP.[87] It was established that the three structural types proposed for the most stable α-form have different packing types of the macromolecule. Therefore, it is not surprising that the calculated energies also differ by 0.5–1.7 kcal mol^{-1}, the differences being larger for the plane wave basis set. According to PW91/340 eV calculations, the β- and γ-polymorphs have nearly equal energies. Interestingly, the calculated stabilities of the polymorphs correlated with their melting points.

VI. Studies of the electronic structure

Most molecular crystals of organic and organoelement compounds are dielectrics whose properties depend only slightly on the band gap.[12] As a rule, DFT calculations with GGA functionals underestimate the band gaps for semiconductors and dielectrics. In spite of this, analysis of the electronic structure is of great importance for the search for novel promising materials, in particular, for optoelectronics. The main method of investigation of the electronic structure is to analyze the density of states, the energy band structure and the calculated absorption spectra in order to determine the contributions of particular orbitals or functional groups to these properties. This makes it possible to assess the mechanism of optically induced charge transfer in the crystal.

For a glycine/sodium nitrate mixed crystal, the calculated absorption edge is shifted by 20–50 nm towards the long-wavelength region compared to the experimental data.[88] Calculations using the PW91 functional give a larger shift compared to the LDA functional. Both functionals predict that the crystal under study is a semiconductor with a band gap of 2.9 eV.

A complex of 4-hydroxypyridine-2,6-dicarboxylic acid and $Cu_2(OH)_2CO_3$ is a one-dimensional coordination polymer (Fig. 3). The hydrogen bonds O–H···O link polymer chains to form a three-dimensional network.[89] Experiments

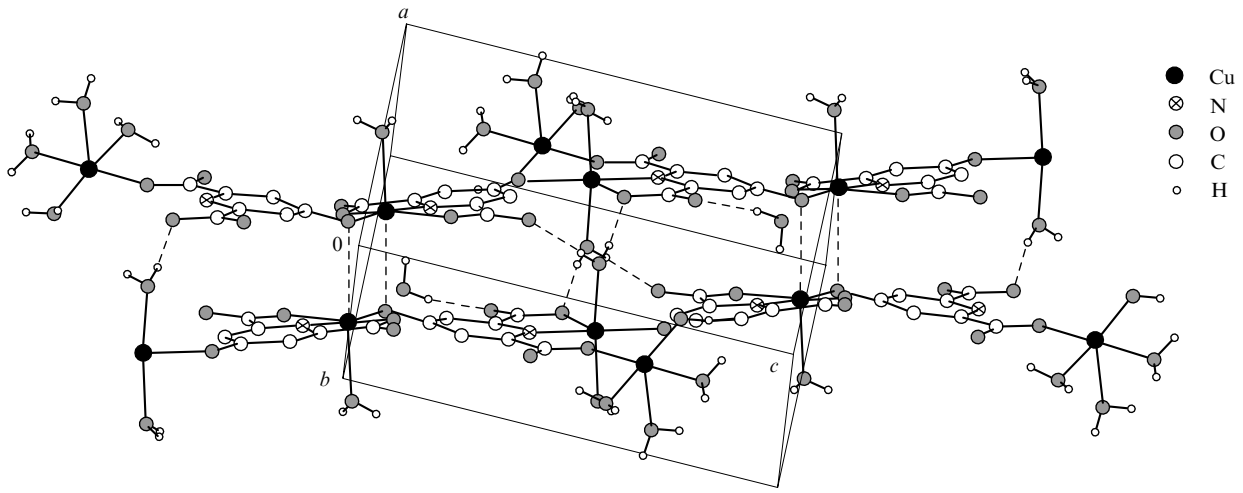
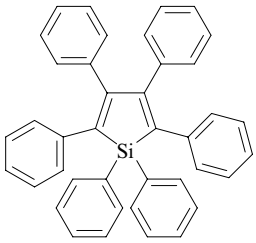


Figure 3. Fragment of crystal packing of the complex of 4-hydroxypyridine-2,6-dicarboxylic acid with $Cu_2(OH)_2CO_3$.[89]

revealed that the material emits luminescence (a band at 379 nm) and has a band gap of 2.85 eV. Quantum chemical calculations using the PBE functional gave a smaller band gap value (1.89 eV). A band corresponding to electron density transfer from the Cu 3d sublevel to C and O 2p sublevels was localized at 374 nm, which differs from the experimental value by merely 5 nm. An important role of quantum chemical calculations of crystals was clearly demonstrated in a study of the mechanism of electron transfer in 1,1,2,3,4,5-hexaphenylsilole (**59**) which can be used as material for light-emitting substrates in organic light-emitting diodes.



59

A total of nine variants of electron and hole transport involving their local environment in the crystal were considered.[90] A study of the energy band structure of compound **59** showed that the highest mobility of holes should be expected along the *ab* plane of the unit cell. Holes are characterized by higher mobility than electrons. Quantum molecular dynamics simulation with inclusion of the influence of temperature and pressure showed that **59** can be most efficiently used in organic light-emitting diodes in the temperature range from 243 to 343 K.

Considerable literature is devoted to the mechanism of electron density transfer, in particular, to search for the corresponding crystallographic direction. Often, these directions are governed by motifs of crystal packings formed through hydrogen bonds, stacking or other intermolecular interactions in crystals. For instance, such studies were carried out for two polymorphs of compound **58**,[91] **50**,[92] pentacene,[93,94] tetracene,[94,95] poly(3,4-ethylenedioxythiophene),[96] perylenediimide,[97] α-2-methyl-1-nitrosothiourea,[98] mixed crystals of copper(I) sulfites with organic ligands,[99] and hybrid organic-inorganic materials with the perovskite structure.[100] Almost all calculations were carried out using conventional non-hybrid functionals (except Ref. 95); however, the results obtained were in reasonable agreement with experimental data.

A coordination polymer $[Cu(HF_2)(pyz)_2]BF_4$ (pyz is pyrazine), which exhibits the properties of an antiferromagnet, appeared to be difficult to study.[101] The superexchange between copper atoms involves the HF_2 groups. It is believed that the superexchange can occur by either the mechanism of spin polarization of H and F atoms or axial overlap of $Cu(\uparrow) - Cu(\downarrow)$ states. The best fit to experimental data was obtained using a hybrid functional with a contribution of the 'exact' (Hartree-Fock) exchange potential (F_x) from 20% and 35%. In the latter case, not only the unit cell parameters, but also the antiferromagnetic-to-paramagnetic transition temperature and the superexchange constants were reproduced more correctly. Calculations with $F_x = 20\%$ led to significant differences of the calculated parameters from experimental values. It should be noted that the Mulliken atomic charges and the forbidden gap values differed insignificantly at both F_x values (20% and 35%).

Usually, software for analysis of the electron density redistribution between atoms is only suitable for analysis using the Mulliken scheme and analysis of the density of states. Other schemes of calculations of charges in isolated molecules [*e.g.*, the Natural Bond Orbital (NBO) scheme][102,103] are ignored. At the same time, it is possible to carry out topological analysis of the electron density distribution according to Bader's theory 'Atoms in Molecules'[104] using, *e.g.*, software developed by independent vendors not related to the programmer teams working on software for quantum chemical calculations of crystals.

VII. Topological analysis of the calculated electron density of crystals

Topological analysis of the electron density distribution aimed to study the nature of chemical bonds in crystals faces some difficulties. The software for topological analysis of the electron density distribution was mainly developed for work with analytical representation of the function $\rho(\boldsymbol{r})$

(programmes AIMPAC,[105] AIM2000,[106] MORPHY,[107] TOPMOD,[108] AIMALL,[109] DENPROP[110]) and does not allow one to use periodic boundary conditions and/or plane wave basis sets. Here, 'analytical representation' means knowledge of information on the orbitals in the crystal (*i.e.*, knowledge of all coefficients in the expression describing the molecular orbital). Probably, the only exception is the TOPMOD programme[111] developed to manipulate the output data of the programme CRYSTAL. The method used in many studies based on quantum chemical calculations using various versions of the programme CRYSTAL is as follows. First, the X-ray structural factors are calculated theoretically. Then, they are used in the refinement procedure within the framework of the Hansen–Coppens multipole model[112] provided that relevant software, *e.g.*, XD2006 (Ref. 113) is available. Usually, the results obtained are compared with experimental X-ray diffraction data on the electron density distribution. This approach is inconvenient because some efforts should be made to transform the calculated structural factors to a form suitable for further multipole refinement. This requires additional data that cannot be obtained by quantum chemical methods, *e.g.*, parameters of anisotropic atomic displacements (thermal parameters) and the standard deviations of all structural factors. Mathematical tools for obtaining the necessary values from neutron diffraction data were reported by Brunning and Feil.[114] Then, these tools were used to study an urea crystal.[115]

Considering software using the plane wave basis sets and pseudopotentials, the only possibility to carry out topological analysis of the function $\rho(\boldsymbol{r})$ is to represent it in a numerical form as a discrete array of numbers related to the cell coordinates. Files containing arrays of numerical data can be extracted from any programme for quantum chemical calculations. Software that can manipulate these data include DGrid,[116] AIM (a component of the ABINIT software package),[117] Bader (only calculations of charges),[118] InteGriTy,[119] EXCUBO,[120] GRID.[121] The results of calculations depend on the density of point distribution in the array.

Yet another serious problem is associated with the pseudopotentials *per se*. It is believed that the use of pseudopotentials precludes a correct topological analysis of the electron density distribution owing to the appearance of 'strange' critical points in the action range of the pseudopotentials.[122–125] In other words, if position of a $(3,-1)$ critical point falls within the action range of the pseudopotential, either this critical point will not be located or other types of critical points will be located. It was assumed[122–125] that the pseudopotential should be replaced by the electron density preliminarily calculated for an isolated atom, or the function $\rho(\boldsymbol{r})$ should be reconstructed from the pseudopotential. The first method is used in the AIM programme for calculations of atomic charges; it can be recommended for most pseudopotentials. Reconstruction of the function $\rho(\boldsymbol{r})$ in the region of atomic core electrons is implemented in the VASP programme (version 4.6.31 and higher). Carrying out topological analysis in a most correct manner requires information on the type of connection of the pseudowave function to the wave function determined by plane waves. In the PAW formalism, the core is described by a smooth pseudowave function and an augmentation charge sphere of radius R_{aug} (compensation charge). The electron density inside the augmentation sphere is equal to that for the sphere determined by the full-electron wave function and can be obtained by integration. The main goal of this procedure is to calculate the atomic charges. Unfortunately, such a 'reconstructed' function $\rho(\boldsymbol{r})$ incorrectly reproduces the electron density distribution function.

Thus, if a $(3,-1)$ critical point is inside the augmentation charge sphere, it will probably not be located. At the point R_c (pseudopotential cutoff), the value of a smooth pseudowave function equals that of the full-electron wave function (wave function determined by the plane wave basis set). In the region between R_{aug} and R_c, the wave function is determined by three components, *viz.*, a rapidly decreasing function of the augmentation charge, a smooth pseudowave function and the plane waves. In this region, a $(3,-1)$ critical point will be located with certainty.

The problem of location of critical points of chemical bonds and intermolecular contacts can be solved using a pseudopotential with small R_c value (and, correspondingly, R_{aug} in the PAW formalism). The pseudopotential cutoff R_c as well as the size of the basis set depend strongly on the type of the pseudopotential used. When choosing a pseudopotential with small R_c, one should keep in mind that it requires a large basis set. In any case, the PAW method requires a smaller basis set than the pseudopotentials with conservation of normalization. A rather large number of programmes for generation of a necessary pseudopotential is available from the Internet.§ Nevertheless, it should be noted that generation of a pseudopotential for heavy atoms (especially, atoms of f-elements) is a nontrivial problem. In addition, the $(3,-3)$ critical points corresponding to positions of atomic nuclei cannot be located in any cases. The situation with the VASP programme is somewhat better. The software development team provides a variety of relativistic PAW pseudopotentials for almost all elements of periodic system including those characterized by small R_c values. Therefore, the VASP programme is used for quantum topological analysis of the electron density in crystals.

An example of the approach in question is provided by the results of topological analysis of the function $\rho(\boldsymbol{r})$ for a mixed crystal of tetrathiafulvalene and 2,5-dichloro-*p*-benzoquinone (**60**) carried out using the PAW pseudopotentials, the plane wave basis sets (680, 952, 1224 and 1360 eV) and the programme InteGriTy (Fig. 4 *a*).[119] The increment between the points in the array of the $\rho(\boldsymbol{r})$ values varied from 0.07 to 0.0055 Å. To increase the accuracy of calculations, a cubic interpolation procedure was incorporated into the programme InteGriTy. The absolute values of the topological characteristics, namely, the electron density and the Laplacian of the electron density at the $(3,-1)$ critical point, depend only slightly on the size of the basis set and differ in the third or fourth decimal digit. The smallest variations were found for the topological parameters of weak intermolecular interactions; variations at the $(3,-1)$ critical points of single bonds are more pronounced. The Laplacian of the electron density at the $(3,-1)$ critical point of the double bond C=O shows the strongest dependence (in the first decimal digit) on the size of the basis set and on the increment between the points in the data array. In the case of multiple bonds, convergence of results requires an

§ More detailed information can be found at http://www.abinit.org/downloads/psp-links/pseudopotentials.

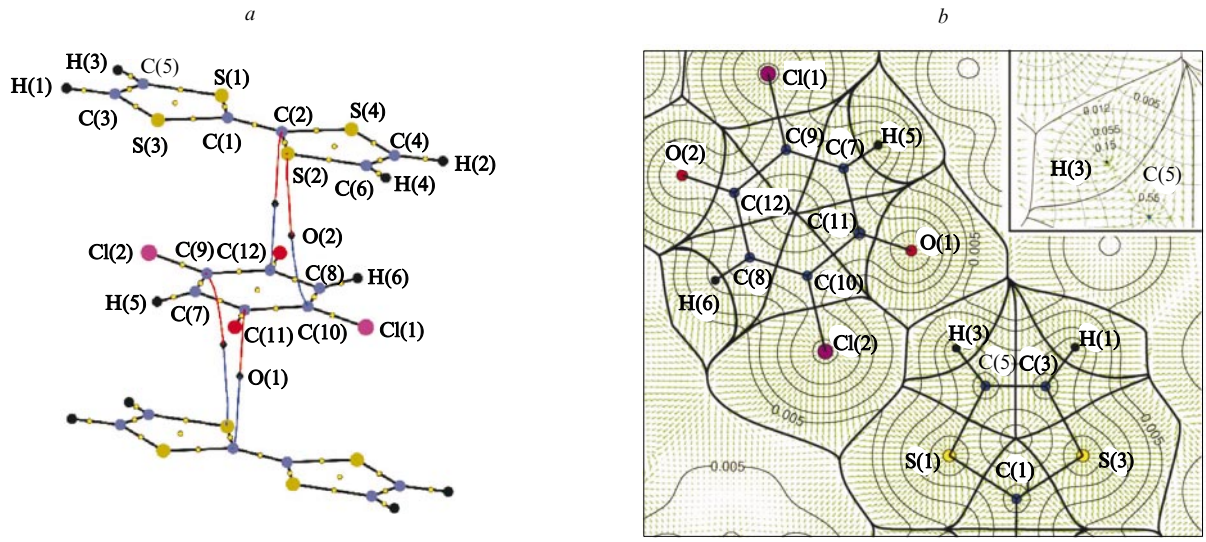


Figure 4. The (3, −1) critical points corresponding to stacking interaction in co-crystal **60** (*a*) and the molecular graph of 2,5-dichloro-*p*-benzoquinone and tetrathiafulvalene fragment (*b*).[119]

increase in the increment to a maximum possible value determined by the size of random access memory. By and large, a maximum of kinetic energy of at most 680 eV is sufficient for estimation of charge transfer from tetrathiafulvalene molecule to 2,5-dichloro-*p*-benzoquinone to an accuracy of 0.02e while an increment of 0.05 Å is sufficient to obtain topological characteristics with an acceptable accuracy (Fig. 4 *b*).[119] Thus, topological analysis of the electron density distribution for molecular crystals does not require a large basis set and a large array of numerical values of the function $\rho(\boldsymbol{r})$. The corresponding file sizes are of the order of a few hundreds of megabytes and can be processed in a rather short time.

The study by Souhassou and co-workers[119] is not the only example of numerical computation of topological characteristics of the electron density distribution for organic and organoelement compounds. In particular, topological analysis was carried out for crystals of 1-hydrosilatrane (**61**),[126] 1-fluorosilatrane (**62**),[127] two tris(pentafluorophenyl)silylamines (**63** and **64**),[128] two cyclic organylfluorosilanes (quasi-silatranes **65** and **66**),[129] molecular complexes of *o*-phenylenemercury with ethanol and tetrahydrofuran solvate molecules (**67** and **68**),[130] two rhodacarboranes (**69** and **70**),[131] chloridobis[(2-oxoazocan-1-yl)methyl]germanium(IV) trifluoromethanesulfonate (**71**),[132] three C,O-chelate complexes of germanium(IV) (**72**–**74**),[133] complexes of tris(pentafluorophenyl)silanes with Lewis bases (**75**–**78**),[134] (amidomethyl)dimethylsilanol hydrohalides (**79** and **80**)[135] and a donor-acceptor complex $PPh_3 \cdot AuCl$ (**81**).[136] Optimization was carried out using the PBE functional, the maximum kinetic energy ranged from 400 to 680 eV, and points in the numerical data array were separated by less than 0.04 Å. This functional was chosen because a large number of transferable PAW pseudopotentials with small R_c values are available. For all these crystal structures, the energies of weak intermolecular interactions and coordination bonds involving atoms of Group IVA elements were estimated using the Espinosa–Molins–Lecomte empirical correlation[137–139] which relates the potential energy density $[V^e(\boldsymbol{r})]$ at the (3, −1) critical point to the C−H···O, N−H···O and O−H···O interaction energies,

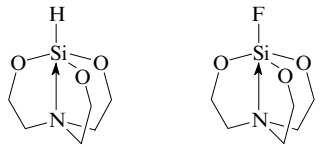
$$E = 313.75 V^e(\boldsymbol{r}) \text{ [kcal mol}^{-1}\text{]} . \quad (16)$$

Relation (16) was applied[126–136] to describe hydrogen bonds of different strength (energy > 15 kcal mol^{-1}), coordination bonds involving metals atoms and atoms of Group IVA elements, and to estimate the sublimation energy at 0 K as the total energy of all intermolecular interactions. Note that the accuracy of the energy values obtained using relation (16) and the applicability range of this relation are unknown.

Crystals of compounds **66**, **79** and **81** were studied by not only quantum chemistry methods, but also by high-precision X-ray diffraction analysis. Therefore, it is appropriate to compare the values of the electron density and the Laplacian of the electron density at the (3, −1) critical points of the chemical bonds and intermolecular contacts obtained from quantum chemical calculations with results of multipole refinement. Differences may be due to at least mismatch of the experimental and optimized atomic coordinates. The largest differences (up to 60%) between the values of the Laplacian of the electron density were obtained for nonpolar covalent bonds; differences in the electron density values are smaller (∼2%–10%).

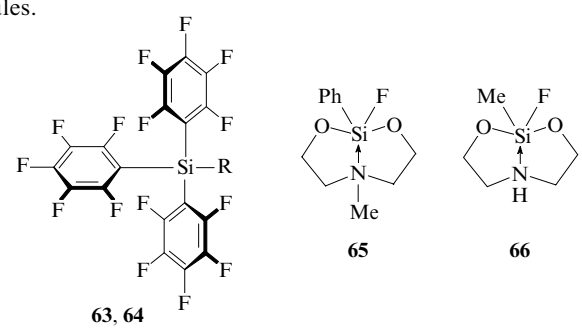
The geometries of molecules **61** and **62** in the crystals are noticeably different from those in the gas phase. In particular, the intramolecular coordination bond Si−N in the crystals of the compounds is 0.25 Å shorter than in the gas phase (according to gas-phase electron diffraction data).[140, 141] Topological analysis of the electron density distribution revealed the onset of numerous intermolecular interactions C−H···O in the crystal and the changes in the atomic charges of oxygens. This leads to redistribution of the electron density in the coordination site of silicon atom and to a corresponding shortening of the Si−N bond. In particular, the total energy of C−H···O intermolecular

interactions (hydrogen bonds) in the crystal of compound **61** is 55% of the sublimation energy.



61 **62**

The energies of the coordination bond Si—N in crystals **61**, **62**, **65** and **66** evaluated using relation (16) range from 18 to 29 kcal mol^{-1}. According to B3LYP/6-311G(d) calculations,[142] the coordination bonds Si—N in crystals **61** and **62** are 10–12 kcal mol^{-1} stronger than in isolated molecules.

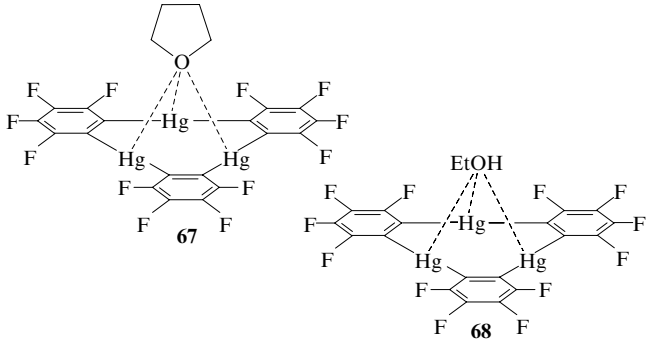


63, **64**

R = NHBn (**63**), (**64**).

In compounds **63** and **64**, the structure-forming interactions F···F are of the 'hill–valley' type.[104] In other words, they are characterized by orientation of the lone electron pair of one fluorine atom towards the region of electron density depletion of fluorine atom of the adjacent molecule (Fig. 5). An important role is also played by the stacking interactions between phenyl and pentafluorophenyl groups. The crystal packing of compound **63** shows no infinite stacking motif, thus being looser than that of **64** [according to X-ray diffraction data, the densities of the silanes are 1.669 (**63**) and 1.805 (**64**) g cm^{-3}]. The looser packing is characterized by a lower sublimation energy than the more dense packing (10.9 and 17.8 kcal mol^{-1}, respectively, as obtained from calculations).

In crystals **67** and **68**, oxygen atoms of tetrahydrofuran and ethanol solvent molecules participate in three interactions with mercury atoms. Among them, only one interaction can be considered as weak coordination bond [its energy is 7.1 (**67**) and 7.6 (**68**) kcal mol^{-1}, and the Hg—O



67 **68**

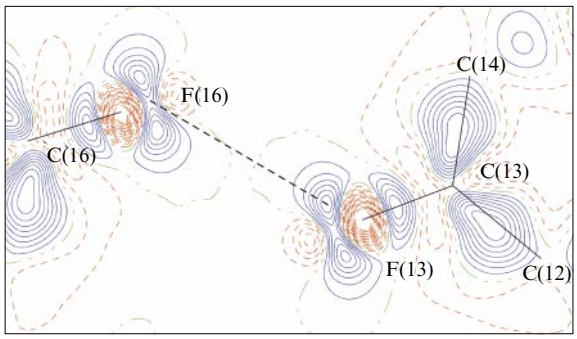
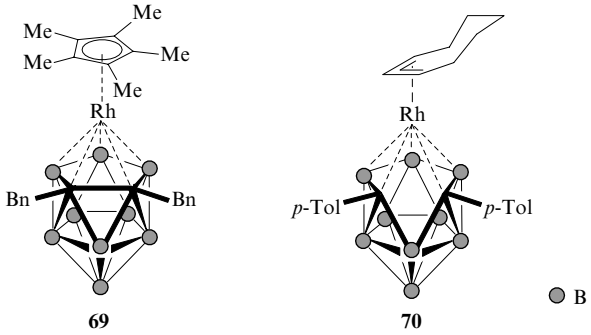


Figure 5. The calculated deformation electron density distribution in the region of intermolecular contact F···F in the crystal of compound **63**.[104]

interatomic distances are 2.910 (**67**) and 2.872 (**68**) Å], the energies of other interactions being much lower (~1 kcal mol^{-1}).[130] Mercury atoms complete their coordination spheres through a variety of weak intermolecular contacts Hg···F and Hg···H with energies no higher than 1 kcal mol^{-1}.

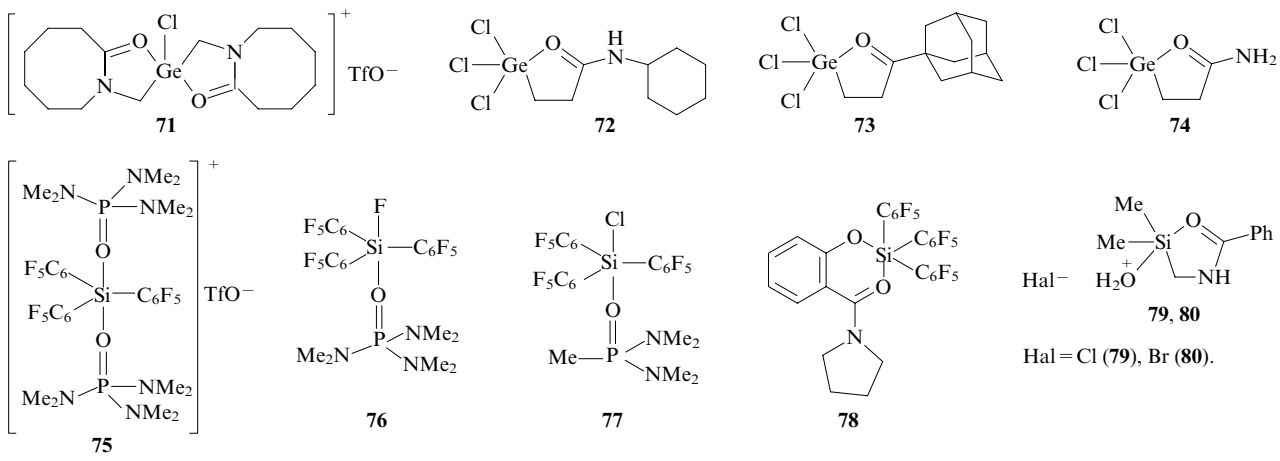
An analysis of the atomic charge values calculated for two rhodacarboranes **69** and **70** according to Bader revealed changes in the valence electron density distribution in the metallacarborane cage. Cleavage of the C—C bond leads to a decrease in the positive charge on rhodium atom by 0.07 e; this is accompanied by a significant increase in the negative charges on carbon atoms of the carborane cage (by 0.4 e).[131]



69 **70**

In crystal **71**, the distance between the germanium atom and the oxygen atom of triflate ion is 3.433(2) Å, being less than the sum of the corresponding van der Waals radii (from this point on, coordination bonds in the formulas of compounds are shown as conventional single bonds).[143] The Ge—Cl bond lying opposite to triflate anion is somewhat longer than the corresponding bonds in this class of compounds. The aim of analysis of the calculated function $\rho(\boldsymbol{r})$ was to determine whether or not the Ge—O interatomic distance corresponds to a weak coordination bond. Eventually, no coordination bond was revealed and it was concluded that only C—H···O interactions with energies 0.9–1.9 kcal mol^{-1} occur between the cation and anion.[132]

In crystals of complexes **72**–**74**, the intramolecular coordination bonds Ge—O are 0.08–0.18 Å shorter than in isolated molecules. Topological analysis of the calculated electron density distrbution functions of these crystals (PBE/400 eV) and isolated molecules showed that in the solid phase the Ge—O bond is stronger than in the gas



phase (its energy is 5–11 kcal mol^{-1} higher). Interestingly, a noticeable contribution to the sublimation energy (~20%) comes from intermolecular interaction between the electron pair of chlorine atom and the antibonding orbital of the C=O bond.

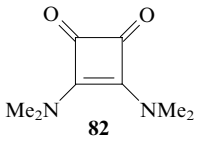
Evaluation of the energies of the coordination bonds in crystals **75**–**78** containing five-coordinate silicon atoms showed that bonding in the O–Si–O and O–Si–X [X = F, Cl, C_6F_5, O=P(NMe$_2$)$_3$] fragments corresponds to the three-centre four-electron bond with the Si–O and Si–Hal bonds having nearly equal energies. A similar conclusion was drawn for salts **79** and **80**.

In the case of crystal $PPh_3 \cdot AuCl$ (**81**) the results of topological analysis of the calculated electron distribution function were compared with the results of high-precision X-ray diffraction experiment.[115] Calculations with the PBE functional correctly reproduced the topological characteristics of Au–Cl and Au–P bonds, the energy difference being at most 2 kcal mol^{-1}. The calculated total energy of all interactions involving the gold atom was almost equal to the experimental value (*cf.* 3.4 and 3.3 kcal mol^{-1}, respectively).

Reproduction of atomic charge values appeared to be a more complicated task. The impossibility of taking into account core electrons in explicit form may have a negative effect on the results of integration of the function $\rho(\boldsymbol{r})$. Nevertheless, the results of calculations of a crystal of salt **81** appeared to be in reasonable agreement with the results of multipole refinement of X-ray diffraction data, *viz.*, the atomic charges of Au, P and Cl were 0.045, 1.737 and −0.782 e, respectively (*cf.* the corresponding experimental values of 0.003, 1.135 and −0.963 e).

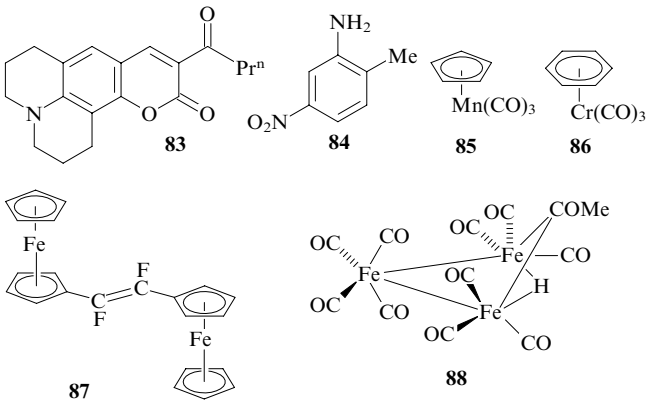
Taking compounds **63** and **64** as examples, it was shown that the type of a pseudopotential has no decisive effect on the results of topological analysis of the function $\rho(\boldsymbol{r})$ in the case of Group I–III elements. As to heavier elements, topological analysis of the electron density distribution was carried out for Au, Rh and Hg and satisfactory results were obtained. Meanwhile, topological analysis using analytical form of the function $\rho(\boldsymbol{r})$ is difficult because localized full-electron basis sets for these elements, which correctly describe the properties of corresponding organoelement compounds, are available for a few software packages (*e.g.*, ADF).[16]

Topological analysis of the function $\rho(\boldsymbol{r})$ was also performed in order to explain an unexpectedly large increase in the dipole moment of the molecule of 3,4-bis(dimethylamino)cyclobut-3-ene-1,2-dione (**82**)[144] on going from the gaseous to crystalline state (from 7.3 to 12.6 D). Quantum chemical calculations were carried out by the Hartree–Fock method with the 6-21 G basis set; however, they played a supportive role and the results obtained were not considered in detail.



Vener *et al.*[145] reported the results of a much more representative B3LYP/6-31G(d,p) study of 26 molecular crystals with strong hydrogen bonds. No structure optimization was done. The available structural data were used 'as is' without analyzing their quality. At the same time, the results of quantum chemical calculations of isolated molecules and ions with geometry optimization were also reported. Since differences in the geometric parameters of the fragments with strong hydrogen bonds O–H···O and N–H···O in isolated molecules, ions and crystals are small, the corresponding differences in the $\rho(\boldsymbol{r})$ and $\nabla^2\rho(\boldsymbol{r})$ values are usually also small. This first of all indicates that the differences are due to the influence of crystal packing and possible experimental errors in the determination of positions of hydrogen atoms. A more reliable conclusion can be done after optimization of atomic coordinates in the crystal using different methods and basis sets. In addition, topological parameters can be compared with the results of calculations for isolated molecules or clusters.

A more developed approach to analysis of the calculated electron density distribution function described in the beginning of this Section was used for the first time in a study of urea crystal.[115] Seemingly, it served as a base for subsequent experimental and theoretical investigations of crystals of two polymorphs of the dye coumarin 314 (**83**),[146] 2-methyl-5-nitroaniline (**84**),[147] and π-complexes (η^5-C_5H_5)Mn(CO)$_3$ (**85**), (η^6-C_6H_6)Cr(CO)$_3$ (**86**), (*E*)-{(η^5-C_5H_4)CF=CF(η^5-C_5H_4)}(η^5-C_5H_5)$_2$Fe$_2$ (**87**)[148] and the cluster Fe$_3$(μ-H)(μ-COMe)(CO)$_{10}$ (**88**).[149] Emphasize that the atomic coordinates in structures **83**–**88** were not optimized (experimental data were used).



In a study[125] of two polymorphs of the dye **83**, optimization of atomic coordinates by the B3LYP/6-31G(d,p) method led to shortening of the interatomic distances corresponding to intermolecular contacts by 0.01–0.05 Å. It is not surprising that the calculated values of their energies estimated using relation (16)[137–139] also appeared to be much higher than the experimental values. Although the calculated heats of sublimation (32 and 41.3 kcal mol^{-1}) differ from experimental values (36.3 and 38.7 kcal mol^{-1}, respectively), they are in qualitative agreement with the order of the relative stabilities of the polymorphs. The experimental topological parameters of compound **84** and those obtained from HF/6-31G(d,p) calculations are also in good agreement. Nevertheless, there has been a trend towards an increase in the $\nabla^2\rho(\boldsymbol{r})$ values and a decrease in the ellipticity at the $(3,-1)$ critical points of covalent bonds.

Quantum chemical calculations were used to confirm an experimental model of chemical bonding in various transition metal π-complexes based on X-ray diffraction data.[148] Crystals of the complexes **85** and **86** represented complex objects for multipole refinement because their theoretical and experimental connectivity graphs showed some mismatch. This was explained by specific features of the electron density distribution in the vicinity of Mn and Cr atoms. A high-precision X-ray diffraction study of the electron density distribution in the crystal of cluster **88** faced similar difficulties. Probably, the character of the distribution in the vicinity of metal atoms [curvature of the function $\rho(\boldsymbol{r})$] is strongly dependent on the refinement procedure and correct reproduction of its features using computational methods alone is impossible.

From the aforesaid it follows that the number of studies on the topological analysis of the calculated function $\rho(\boldsymbol{r})$ in crystals of molecular compounds is not so large. Quantum chemical calculations play a supportive role; they are mainly carried out in order to confirm the results of high-precision X-ray diffraction studies.

VIII. Estimates of NMR and EPR spectroscopic characteristics

Would quantum chemical calculations be applied to compute the magnetic shielding and quadrupole moment tensors, solution of many problems related to the interpretation of the NMR and EPR spectra of solids could be essentially simplified. However, this is a complicated problem. To reproduce the experimental chemical shifts, one should describe as accurately as possible the state of atomic core electrons and the component of the wave function responsible for the 'behaviour' of valence electrons in the core region. These requirements are met by the programme CRYSTAL which includes multiply split full-electron basis sets for the period 1 to 5 elements.¶ However, this programme, like all other programmes that use localized basis sets, has no functional possibilities for performing this type of calculations. As might appear, the plane wave basis sets and pseudopotentials are inappropriate for calculations of the magnetic shielding and quadrupole moment tensors. However, in practice only the programmes with these basis sets are used for calculations of NMR and EPR spectra.

The magnetic shielding of an atomic nucleus by electrons (σ_i) is a tensor quantity, *i.e.*, it depends on the orientation of a molecule or crystal relative to the direction of external magnetic field. The chemical shift (δ_i) can be defined as the difference between the shielding for a reference compound (σ_{ref}) and the shielding for the compound under study (σ_i)

$$\delta_i = \frac{\sigma_{ref} - \sigma_i}{1 - \sigma_{ref}}. \qquad (17)$$

Components of the magnetic shielding tensor $\sigma_{\alpha\beta}$ can be defined as partial derivatives of the total energy of a molecule with respect to the magnetic field strength (B) and to the intrinsic magnetic moment of the atomic nucleus (μ)

$$\sigma_{\alpha\beta} = \frac{\partial^2 E}{\partial m_\alpha \partial B_\beta} = \frac{\partial^2 E}{\partial B_{\beta\alpha}} \neq \frac{\partial^2 E}{{}_\beta\partial B_\alpha} \neq \sigma_{\beta\alpha}. \qquad (18)$$

Generally, the magnetic shielding tensor is asymmetric, *i.e.*, permutation of the indices α and β gives a different result. The $\sigma_{\alpha\beta}$ values are calculated using a perturbative approach.[150] When calculating the chemical shifts using pseudopotentials, it is assumed that the amount of electron density in the region described by the pseudowave function is always constant. Then, one can assume that the contribution of the pseudowave function is small and ignore it or try to reconstruct the full-electron wave function from the pseudowave function. Such a reconstruction was carried out for the first time taking calculations of EPR spectra of semiconductors as an example,[151] because theoretical approaches to calculation of the quadrupole moment tensor and EPR spectroscopic parameters are similar to the case for NMR. Thus, there are two general procedures for calculations of the chemical shifts in NMR spectra.

The least efficient procedure is incorporated into the CPMD programme in which the magnetic shielding and quadrupole moment tensors are calculated ignoring core electrons. The behaviour of the wave-function component responsible for valence electrons in the core region is also ignored. Therefore, the software development team† recommend to consider the results of calculations for atoms of the period 3–6 elements with care. By and large, calculations of the chemical shift require much larger basis sets (maximum values of the kinetic energy) compared to those used in the geometry optimization and in calculations of

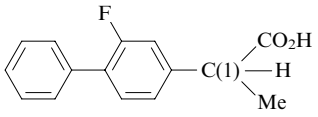
¶ Visit http://www.crystal.unito.it/Basis_Sets/Ptable.html.
† Visit http://cpmd.org/documentation/cpmd-html-manual.

most other properties. For hydrogen atoms, a basis set of the order of ~1000 eV is large enough. Calculations of δ^{29}Si require a maximum kinetic energy of at least 8000 eV.[152]

Detailed comparative results were obtained in a study[153] of amino acids and their hydrates. Very good agreement with experimental data (at least 1.5 ppm) was obtained for the hydrogen atoms involved in strong hydrogen bonds N—H···O and O—H···O. The calculated signals (δ) of the hydrogen atoms of phenyl and methylene groups are shifted to lower field by 1.6–5.1 ppm (2 ppm on the average). Interestingly, these differences were first of all explained by the influence of thermal motions.[153] The introduction of the van der Waals correction did not lead to significant changes in the chemical shifts. Analogous results were also obtained and for a proton-conducting crystal of imidazole-bis(ethylene oxide)-imidazole.[154]

The Gauge-Included Projected Augmented Wave (GI-PAW) method[155] is an improved technique which takes account of the behaviour of valence electrons in the core region using some additional localized functions. This allows one to reconstruct the full-electron wave function and to correctly describe the shielding of the atomic nucleus. Emphasize that this requires the use of specially developed pseudopotentials. GI-PAW quantum chemical calculations can be performed using the programmes CASTEP and Quantum ESPRESSO (see Table 1). For organic compounds Deviations of the ^{1}H chemical shifts from the experimental values (2.9 ppm, Ref. 156) are in fact equal to those obtained using a less efficient algorithm incorporated in the programme CPMD. These deviations can be due to thermal motion of atoms in the crystal and to mismatch of the optimized and experimental geometries of the structures under study. An undoubtful advantage of the GI-PAW method is the possibility to estimate with good accuracy the chemical shifts of atoms of the second-period elements and even heavier atoms. That is why GI-PAW is very popular among the methods used for calculations of crystals of various inorganic compounds.[157]

Obtaining δ^{13}C values with high accuracy requires calculations of the chemical shifts using experimental structural data (neutron diffraction data are most appropriate) as the initial approximation and optimization of atomic coordinates. By comparing the calculated and experimental chemical shift values one can establish the source of deviations; the accuracy of calculations can be increased upon subsequent statistical processing of data. The ^{13}C chemical shifts for fourteen carbohydrates and aromatic compounds were calculated[158] and the results obtained were statistically processed. Using neutron diffraction data as the initial approximation without geometry optimization, the average values of the root-mean-square deviations were 20.2 ppm for carbohydrates and 16.8 ppm for aromatic compounds, thus being at least two times better than the results obtained in the calculations with the 6-31G(d,p) basis set. Using an improved original procedure, the accuracy of calculations was increased to 1 ppm.[158] Further increase in accuracy can be attained using the method of *ab initio* molecular dynamics, namely, calculations of the chemical shifts followed by averaging for configurations near the equilibrium state allow the influence of thermal motion of atoms to be taken into account. Taking dipeptide β-L-aspartyl-L-alanine as an example,[159] it was shown that the δ^{13}C values obtained from conventional calculations and by the method of molecular dynamics in the Born–Oppenheimer approximation can differ by a few ppm.

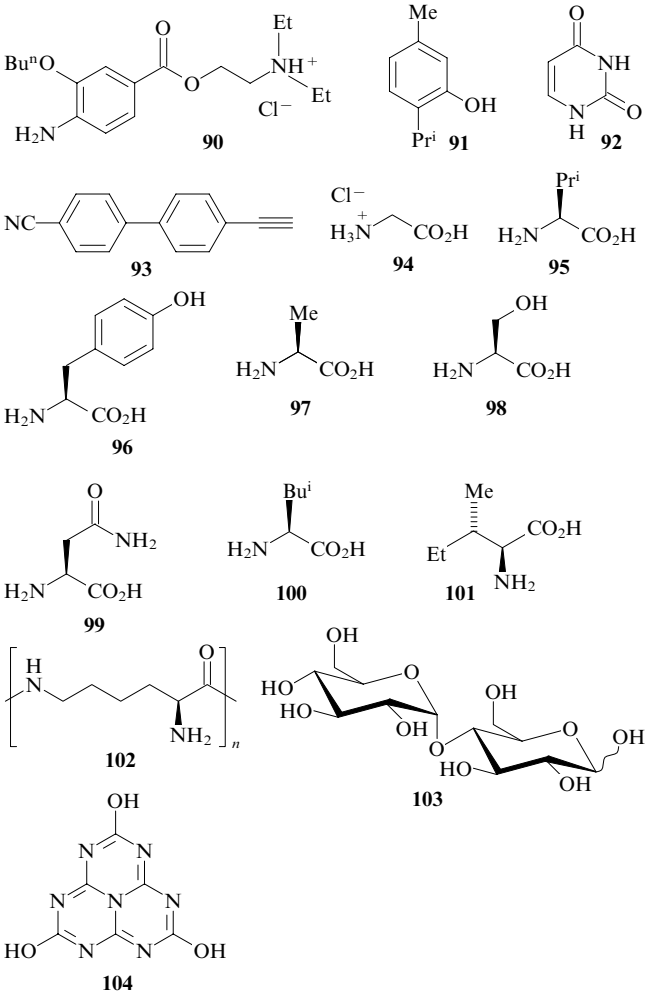


89

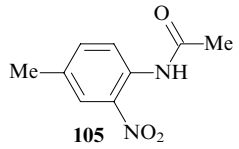
The difference between the calculated and experimental ^{19}F chemical shift values obtained for crystal of fluorobiprofen (**89**) was 2.9 ppm.[160] The authors of that study recommended to carry out optimization of atomic positions regardless of the experimentally determined geometry. For example, the calculated C=O bond length in compound **89** is 0.035 Å larger than the experimental value, while the bond between C(1) and methyl carbon atoms is 0.033 Å shorter. The influence of thermal motion of atoms on the bond lengths can be strong enough even at 150 K (the temperature at which the structure of **89** was studied). At the same time, these differences can be to some extent due to drawbacks of the PBE functional used for calculations. Probably, this is the reason why only positions of hydrogen atoms were optimized.[160]

A remarkable example is provided by investigations of perfluoronaphthalene[161] for which the difference between the calculated and experimental chemical shift values was about 2 ppm. However, calculations overestimate the differences between the δ^{19}F values for fluorine atoms at the C_α and C_β atoms by 2–4 ppm. Full optimization of atomic positions did not significantly improve the agreement between the experimental data and results of calculations. Interpretation of experimental data using two-dimensional (2D) NMR spectroscopy is also ambiguous, *viz*., signals of fluorine atoms in different positions can hardly be distinguished even using 2D NMR spectra. The results of quantum chemical calculations at least do not contradict the 2D NMR spectra and the signals of fluorine atoms at adjacent C atoms can be reliably identified by a combining these methods.

Quantum chemical calculations of the chemical shifts were used also in studies of the structures of oxybuprocaine hydrochloride (**90**),[162] thymol (**91**),[163] uracil (**92**), 4-cyano-4′-ethynylbiphenyl (**93**), glycine hydrochloride (**94**),[164, 165] valine (**95**), tyrosine (**96**), alanine (**97**),[166] serine (**98**), asparagine (**99**), leucine (**100**), isoleucine (**101**) and peptides based on them,[167] poly-L-lysine (**102**),[168] maltose anomers (**103**),[169] and cyameluric acid (**104**).[170] Not only did the authors of these publications compare the experimental data and the results of calculations of the ^{1}H and ^{13}C chemical shifts, but also undertook attempts to construct correlations between the components of the magnetic shielding tensor and various structural parameters. The calculated ^{17}O and ^{15}N chemical shifts were used to assign the 2D NMR spectra. It should be noted that the calculated and experimental values of the ^{17}O and ^{15}N chemical shifts differ to nearly the same extent as the calculated and experimental values of the ^{19}F chemical shifts. The aim of these publications was to determine the structures of complex biological systems for which crystallographic data cannot be obtained.



Probably, one of the most interesting examples is provided by the use of quantum chemical calculations of chemical shifts in order to search for polymorphs and to analyze their structures. One can assume that application of NMR spectroscopy will help to choose the most stable polymorphs. The number of atomic configurations to be studied is rather large; therefore, additional data obtained by NMR spectroscopy can be useful. An attempt to use a combination of these methods in a study of polymorphs of 4-methyl-2-nitroacetanilide (**105**) was reported.[171]



Two polymorphs of this substance are known, a white and a yellow one. The latter contains two molecules in the independent part of the unit cell. Using calculations of isolated molecule **105** (6-311 + G** basis set), the dependences of the chemical shifts on the torsion angles were plotted. The angles at which the calculated δ^{13}C values are the closest to the experimental data can be used as additional parameters in the search for polymorphs. A comparison of experimental data with the results of crystal structure calculations showed that the ^{1}H chemical shifts in the two independent molecules of the yellow polymorph differ by at most 0.3 ppm. In turn, the differences in the calculated ^{1}H chemical shifts for the white and yellow polymorphs are in good agreement with the corresponding experimental values, although the signals are somewhat shifted to a lower field.

Calculations with inclusion of the van der Waals correction made it possible to choose 23 potential polymorphs of compound **91** from a total of 10 000 test structures.[172] For all of them, the δ^1H and δ^{13}C values were found, the results of calculations were compared with the powder diffraction data and it was shown that the most stable structure does not occur naturally.

Polymorphs of glutaminic acid were characterized[173] by not only the ^{17}O chemical shifts, but also by the calculated components of the quadrupole moment tensor. This allowed the orientations of these components to be determined without sophisticated experiments with large single crystals and specific equipment. Note that the components of the quadrupole moment tensor were calculated by the GI-PAW method.

Exact quantum chemical calculations of the chemical shifts for atomic nuclei of third-period and heavier elements are more difficult-to-perform than calculations for lighter elements. Nevertheless, for organosilsesquioxanes with the cubane-type cage $[RSiO_{1.5}]_8$ (R = H, Me, CH=CH$_2$) the difference between the calculated and experimental δ^{29}Si values and the components of the magnetic shielding tensor appeared to be less than 1 ppm.[174] Very close results were also obtained for the ^{31}P chemical shifts in phenylphosphonic acid.[175] However, agreement between the calculated ^{35}Cl chemical shifts in amino acid hydrochlorides[166] and experimental data is poorer (differences range from 2 to 9 ppm.). Good agreement obtained for the δ^{29}Si and δ^{31}P values is most probably due to the use of specially chosen pseudopotentials. In the case of ^{35}Cl nuclei, the differences can arise from difficulties in reproduction of the experimental structure, especially hydrogen bonds. The influence of hydrogen bonds involving chlorine atom on its chemical shift can be noticeable.

Thus, calculations of NMR spectroscopic parameters are useful when interpreting the experimental NMR spectra. Interest in these studies is responsible for the emergence of the so-called NMR crystallography.[150]

IX. Parameters of vibrational spectra

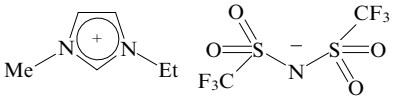
Almost all programmes for calculations of crystal structures allow vibrational frequencies to be calculated. However, only some of them have algorithms for automated analysis of the symmetry of vibrations and for calculations of vibration intensities. Main methods of calculations of vibrational spectra include well-known methods of finite differences and linear response. There is also the 'frozen' phonon method‡ based on the Debye model; it is used to plot the phonon dispersion curves. Eventually, the vibrational spectrum can be calculated using the molecular dynamics methods which give the most accurate values of vibration intensities.

‡ The method is practically implemented as a set of programmes (*e.g.*, PHONON programme).[176] The CRYSTAL09 programme also includes a correction for anharmonicity of vibrations; this allows one to attain good agreement for the frequencies of vibrations involving hydrogen atoms.

Numerous examples of calculations of parameters of vibrational spectra are available in the literature and it is impossible to make a detailed survey of these studies. In the text below we will consider the most interesting examples of the use of calculations for the interpretation of the IR spectra and inelastic neutron scattering spectra as well as the use of phonon dispersion curves. In addition, we will outline calculations of Terahertz vibrational spectra that became popular and on-demand recently.[177–179]

First, it should be noted that almost all calculations are carried out in the harmonic approximation and therefore exact correspondence between vibrational frequencies can not be attained. Despite the fact that calculations explicitly include the effect of crystal packing, the influence of the imperfection of the DFT functionals, thermal vibrations and the use of harmonic approximation introduce noticeable errors into the results of calculations. Nevertheless, analysis of the symmetry of vibrations allows one to avoid limitations intrinsic in the computational methods and makes them a useful tool for the interpretation of experimental data.

Most calculations of vibrational spectra were carried out for crystals of small molecules including amino acids and their salts, 2,6-diamino-3,5-dinitropyrazine,[180] nucleosides and DNA and RNA bases,[181] salts of urea and phosphoric acid,[182] 2,2-bithiophene salts,[183,184] compounds **4** (Ref. 185) and **31**,[186] parabanic acid,[187] co-crystal of glycine and sodium nitrate,[188] cyclohexane-1,3-dione,[188] aliphatic amino acids,[189] formic acid,[28] and NMe_4BF_4.[190] All these studies were aimed to interpret the IR spectra, Raman spectra or inelastic neutron scattering spectra; they include a comparison of the results of crystal structure calculations with the data for isolated molecules. Sometimes, the programmes that use localized basis sets and plane wave basis sets are also compared. The best agreement between the calculated and experimental vibrational frequencies was found in the region from 500 to 1200 cm^{-1}. Consider in more detail the crystal of 1-ethyl-3-methylimidazolium bis(trifluoromethanesulfonyl)imide (**106**) which is transformed to an ionic liquid on melting.

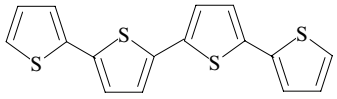


106

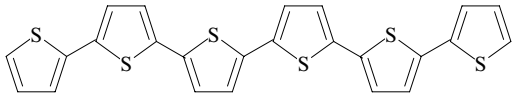
Optimization of atomic positions in crystal **106** (PBE/400 eV)[191] was followed by some shortening of the interatomic distances corresponding to intermolecular contacts and subsequent shift of the frequencies in the range 600–1000 cm^{-1} by a few reciprocal centimetres; the maximum decrease was about 20 cm^{-1}.

In fact, the vibrational frequencies obtained in the crystal structure calculations were always in better agreement with experimental data than the vibrational frequencies of isolated molecules. At the same time, calculations of vibrational spectra of crystals using localized basis sets and the plane waves give close results.

For instance, in a study of some crystalline polymorphs of polythiophene derivatives, namely, α-quaterthiophene (**107**) and α-sexithiophene (**108**),[192] using the programme VASP (PBE/280 eV), all calculations were carried out for a supercell obtained using a doubled minimal lattice constant. This was done to reduce the dependence of vibrational frequencies on the size of the unit cell. To make a comparison of the experimental and calculated inelastic neutron scattering spectra of compounds **107** and **108** the most informative, the vibrational frequencies of compound **108** were normalized to a frequency of 593 cm^{-1} at which the influence of temperature and overtones on the experimental frequencies is minimum. In this case, the vibrational frequencies in the range 600–900 cm^{-1} can be treated as 'fingerprints'; the difference between the calculated values for the two polymorphs of α-quaterthiophene was 10–20 cm^{-1}.



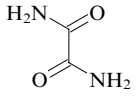
107



108

Ab initio molecular dynamics calculations can be especially useful in those cases where the influence of temperature on the properties of crystals should be taken into account. Examples of such systems are provided by the crystals with strong hydrogen bonds. Molecular dynamics is used to calculate the average values for many-particle systems. The equations of motion are specified for all particles and the average values are obtained by integration over a particular time interval. The principles of *ab initio* molecular dynamics methods have been well documented in a review.[193] The trajectory of the motion of atoms is calculated by quantum chemical methods (most often, within the framework of the DFT); however, atomic nuclei *per se* obey the classical equations of motion. The entire system is in the ground state on the Born–Oppenheimer surface. Particular implementations of methods of *ab initio* molecular dynamics can differ significantly in some details. Nevertheless, in the course of recording of the trajectory (taking into account the fact that the system is near the equilibrium) one can obtain the average values of many properties including those characterizing the changes in the dipole moment. If the trajectory is rather long (at least a few picoseconds), the vibrational spectrum obtained using the Fourier transform of the autocorrelation function of acceleration is representative (free from the influence of random fluctuations).

The experimental inelastic neutron scattering spectrum and the results of molecular dynamics calculations of this spectrum (BLYP/340 eV at 300 K) were compared for the crystal of oxamide (**109**) with N–H···O hydrogen bonds.[194] Calculations correctly reproduce broadening of the lines in the range >900 cm^{-1} and the splitting of the lines at nearly 450 cm^{-1}. However, an attempt to reproduce the range from 1300 to 1800 cm^{-1} in the spectrum of crystal **109** failed because proton was treated as a particle that obeys the classical equations of motion.



109

More subtle effects (electron–phonon, phonon–phonon interactions) and their influence on the spectral pattern can be investigated using the phonon dispersion curves that characterize the changes in the vibrational frequencies along a specified direction of the reciprocal space (anisotropy). A simple example is provided by benzoic acid (**110**).[195] The normal vibrational mode corresponds to deviation of carbonyl group from the plane and shows that dispersion of the vibration is about 30 cm^{-1} (Fig. 6). This allowed one to analyze the lineshape in the experimental inelastic neutron scattering spectrum and to consider the contributions of various exciton components. The phonon dispersion curves of various polymorphs of compounds **107** and **109** showed[192] a noticeable dispersion only for vibrations with frequencies lower than 100 cm^{-1}, which is typical of non-ionic molecular crystals. The phonon dispersion curves can also be used to discuss the detonation processes in energetic materials and to explain the mechanisms of electron transport. Unfortunately, almost no studies of molecular crystals in this field have been reported.

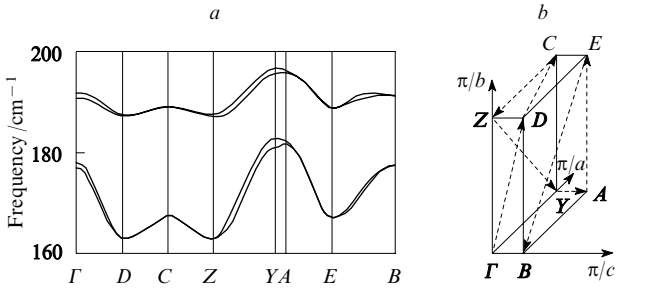
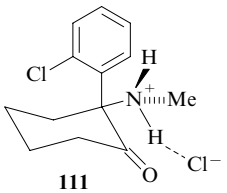


Figure 6. Dispersion curves for low-frequency vibrations of benzoic acid molecules (*a*) and the scheme of points in the Brillouin zone in the crystal of benzoic acid (*b*).[195]

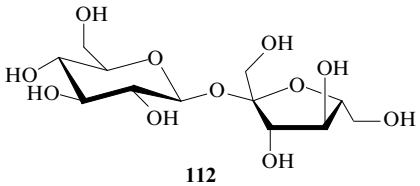
Recently, attention has been paid to absorption spectra in the far IR region (10–200 cm^{-1}) or THz spectra (0.3–6.0 THz)[177–179] in connection with the development of methods and techniques for detection of explosives, narcotics and pharmaceuticals. This frequency range corresponds to lattice vibrations and vibrations corresponding to thermal motion of atoms and molecules in crystals. Therefore, the pattern of the THz spectrum is highly sensitive to the phase state of the substance (crystalline or amorphous; different polymorphs and crystal solvates also have different THz spectra). In addition, the THz spectral pattern is temperature-dependent. Interpretation of corresponding experimental data is intricate. Quantum chemical calculations of vibrational spectra correspond to $T = 0$ K; therefore, one can expect the best agreement with the experiment for the data obtained at the lowest temperature.

Differences in the crystal structures of the L- and DL-forms of compound **98** logically led to different patterns of their THz spectra,[196] which were reproduced using the B3LYP and PW91 functionals with the 6-31G(d,p) and 6-311G(d,p) basis set, respectively. The use of the extended basis set 6-311G(d,p) improves agreement with experimental data; however, the computing time noticeably increases.

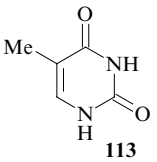
Experimental THz spectra of (*S*)-(+)-ketamine hydrochloride (**111**) were measured at 294 and 78 K.[197] A comparison revealed redistribution of vibration intensities and broadening of lines in the spectra obtained at 294 K. Calculations were carried out with the 6-31G(d,p) basis set and a number of functionals including hybrid ones (BLYP, B3LYP, PW91 and PBE). The best agreement between the results of calculations and experimental data was obtained for the PW91 and PBE functionals. Calculations with the hybrid functional B3LYP gave poorer results. The root-mean-square deviation of peak positions was 3.5 (PW91) and 5.1 (B3LYP) cm^{-1}. Reproduction of band intensities by all functionals was not so good.



111



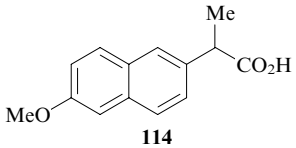
112



113

An analysis of the results obtained in a study of crystals of compounds **111**–**113** allows one to understand why vibration intensities cannot be exactly reproduced.[198] All these crystals contain hydrogen bonds of moderate strength. Quantum chemical calculations in order to obtain vibrational spectra were carried out using a rather large basis set (PW91/1200 eV). For the crystal of compound **110**, the dielectric permittivity and optical polarizability tensors were also calculated. The results obtained suggest a strong correlation between vibrations of the entire molecules and vibrations corresponding to internal degrees of freedom. One can assume that this leads to anharmonicity of vibrational modes in the terahertz range. A similar study of the THz spectrum of benzoic acid revealed the absence of the allowed peak corresponding to rotation of the entire molecule.[199] The spectrum of isolated tetramer of **106** obtained from B3LYP/6-311++G(d,p) calculations exhibited no such peak. Thus suggested[198] that the most accurate reproduction of experimental THz spectra requires a full-electron basis set, taking account of anharmonicity and calculations using supercells (cells obtained using doubled or tripled experimental parameters *a*, *b* and *c*). At present, these requirements are in fact met only when using the CRYSTAL09 programme. Dependence of the results of calculations on the type of the pseudopotential was reported in a study[200] of the crystal of compound **34**. Probably, incorrectly generated pseudopotentials could deteriorate convergence of the equations of the self-consistent field and thus introduce errors into the results of calculations.

A study of 2-(6-methoxy-2-naphthyl)propionic acid (**114**), or the drug naproxen, showed that the introduction of the van der Waals correction has a pronounced effect on the vibrational frequencies.[201]



114

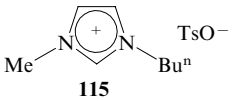
In spite of improved agreement between the calculated [PBE/6-311G(d,p)] and experimental THz spectra upon applying the van der Waals correction, the root-mean-square deviation of the frequencies of the calculated vibrational spectrum from the experimental values appeared to be three times larger than in the case of uncorrected functional PBE (3.8 *vs.* 9.9 cm^{-1}, respectively). The reason consists in drawbacks of the Grimme scheme [63] (see above) that are responsible for overestimation of the energy of dispersion interactions. Because of this the calculated volume of the crystal of naproxen is 10.53% smaller than the experimental value and the vibrational frequencies in the range >90 cm^{-1} are strongly overestimated. Drawbacks of the Grimme scheme were to some extent eliminated using its modification proposed by Civalleri *et al.*[57] In this case, the root-mean-square deviation of the frequencies in the calculated vibrational spectrum from experimental values halved. Note that smaller deviation was obtained when calculations were carried out without rather than with optimization of the cell vectors (4.8 *vs.* 5.5%, respectively). Further improvement can be attained provided thorough choice of the scale factor s_6.

Thus, carrying out test calculations before main calculations may appear to be useful.

X. Dynamic processes in crystals

Consider some examples of the use of quantum chemical calculations to describe phenomena due to thermal motion of atoms in crystals. Problems to be solved by computational methods are related to studies of the vibrational dynamics of molecules and their fragments, dynamic disordering and mechanisms of phase transitions in crystals. However, in these cases the results of calculations should not be treated as reference values because not only the energy considerations, but also various crystallographic characteristics and other properties of crystals (in particular, optical) should be taken into account. This problem is particularly pointed for disordered crystals.

The crystal of 1-n-butyl-3-methylimidazolium *p*-toluenesulfonate (**115**), a precursor of ionic liquid, exhibits ionic conductivity ($\sim 10^{-5}$ S cm^2 at 20 °C);[202] the band gap is too wide for a conductor (2.8 eV at 0 K). This suggested that the ionic conductivity originates from the intense thermal motion of cations and anions at room temperature. Disordering in the crystal of salt **115** is hard to include using only static models for the crystal structure.



115

Among the variety of metallocenes, plumbocene Cp_2Pb (where Cp = η^5-C_5H_5) is the one and only for which crystal structure calculations were carried out.[203] Here, the cyclopentadiene rings are disordered and construction of a correct structural model for the crystal is a complicated problem. The experimental structure is probably a superposition of staggered and eclipsed conformations having close energies. Calculations of different crystal models (PW91/450 eV) with different mutual orientations of C_5H_5 fragments showed that the energy of the crystal structure with molecules in the eclipsed conformation is 2.8 kcal mol^{-1} higher than the energy of this structure with molecules in the staggered conformation. The authors cited [203] believe that the differences are due to intermolecular interactions. Nevertheless, they did not report what is the nature of disordering, namely, static (temperature-independent as, *e.g.*, in ferrocene) or dynamic (temperature-dependent as, *e.g.*, in vanadocene). Also, determination of the space group of the crystal is difficult; in particular, for plumbocene it can be either *Pnma* or $Pna2_1$. Depending on the choice of a particular group the problem of disordering can be to some extent solved. It should be noted that disordering of Cp- or Cp*-ligands (Cp* = η-C_5Me_5) in crystals was observed in many other metallocenes [204–207] which are also characterized by a variety of structural phase transitions associated with rotation of rings.

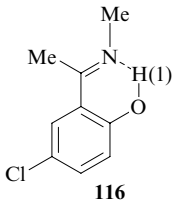
Yet another almost classical example of how uncertainty in the choice of the space group can complicate the interpretation of experimental data and/or results of calculations is provided by potassium hydrogen maleate. According to X-ray diffraction data, this salt crystallizes in the space group *Pnma* (the structure has been a subject of numerous studies, the most accurate data can be found in Ref. 208). However, a feature of this group is a symmetry restriction imposed on position of the central hydrogen atom which participates in the strong intramolecular hydrogen bond O···H···O and occupies a particular position (plane *m*) at the midpoint of the O—O segment. On going to a lower symmetry these restrictions are removed and now the 'disordered' hydrogen atom can occupy two positions on both sides of the plane *m* (pseudoplane in the group $Pna2_1$). This type of hydrogen bonds is well known ('symmetry restricted' bonds). Yet another known example is acetylacetone crystal.[209]

Quantum chemical calculations [208] of the crystal of potassium hydrogen maleate (PW91/495 eV) were carried out using the orthorhombic unit cell determined by X-ray diffraction and no symmetry operations (space group *P*1). Contrary to this, B3LYP/6-31G(d) calculations [210] were carried out using models with experimental values of the unit cell parameters and the space groups *Pnma* and $Pna2_1$. Both calculations gave the same results, *viz.*, removal of crystallographic plane *m* as a result of optimization led to symmetric position of hydrogen atom. This is in good agreement with a flat potential of the O—H···O bond. At the same time, symmetric position of hydrogen atom in isolated maleate anion corresponds to transition state. Taking into account the anisotropy of the thermal ellipsoid of the central hydrogen atom, one can assume its disordering or a larger amplitude of vibrations along the line of the H-bond, which manifests itself as extended thermal ellipsoid. The nature of disordering of the hydrogen atom can be disclosed by carrying out calculations and experiments at different temperatures.

An adduct of quadratic acid and 4,4′-bipyridine is characterized by asymmetric intermolecular hydrogen bond O—H···N.[211] At 453 K, yellow crystals of form I (triclinic crystal system) undergo transition to red crystals of form II (monoclinic crystal system, space group $C2/c$). One more polymorph was obtained after cooling. It is structurally similar to form I (monoclinic crystal system, space group $P2_1/n$. The form I – form II phase transition is accompanied by transfer of hydrogen atom from quadratic acid to bipyridine with the formation of doubly charged anion and cation. *Ab initio* molecular dynamics calculations (PBE/408 eV, $T = 180$, 350 K) were carried out for a supercell obtained by triplication of the smallest lattice constant *a* of form I. It was shown that the energy of the high-temper-

ature form II is 1.1 kcal mol^{-1} lower than that of form I (triclinic polymorph). According to calculations, hydrogen atom does not occupy a symmetric position at the specified temperatures. The averaged O–H distance in form I was 1.27(3) Å, whereas the N–H distance in form II is 1.113(2) Å (numbers in parentheses denote the calculated standard deviation obtained by averaging of the lengths of corresponding bonds for all steps).

There is considerable literature on the dynamics of hydrogen atom in crystals (see, *e.g.*, Ref. 212). Other examples of calculations of crystals of organic or organoelement compounds include calculations of urea–phosphoric acid salt.[213] It should be noted that studies involving molecular dynamics calculations carried out taking into account the anharmonicity of hydrogen atoms are now available. According to calculations of 2-(1-methyliminoethyl)-4-chlorophenol (**116**)[214] with the hydrogen bond O–H···N, taking account of the anharmonicity leads to significant changes in the location region of hydrogen atom H(1). In turn, the interval for the N–O bond length (2.39–2.65 Å) changed as compared to the N–O bond length interval obtained ignoring ananharmonicity (2.39–2.73 Å).



116

Quantum chemical calculations by the Car–Parinello molecular dynamics method were carried out for solid nitromethane[215] to determine the barrier to rotation of the methyl group. A supercell obtained by doubling of one lattice constant was then used for calculations (BP/476 eV, $T = 300$ K). The rotational potential of methyl group has a conventional form

$$V(\theta) = \frac{1}{2} V_3 (1 - \cos 3\theta) ,$$

where V_3 is the barrier to rotation and θ is the angle of rotation.

The coefficient V_3 corresponding to rotation of methyl group by 60° at 0 K equals 0.54 kcal mol^{-1}. At 300 K, the barrier increases to 0.86 kcal mol^{-1}. It is believed[215] this is due to correlations between rotational motion of methyl group and the temperature fluctuations of the environment.

A molecular dynamics study[216] on the decomposition kinetics of pentaerythritol tetranitrate **34** showed[216] that quantum chemical calculations can be used to investigate fast nonequilibrium processes accompanied by rupture of chemical bonds. PBE/DZ calculations were carried out for a tetragonal cell corresponding to experimentally determined parameters. During 500 fs after beginning of the process, compound **34** completely decomposed. The collision rates of molecules along different crystallographic directions were calculated and the kinetic parameters of decomposition were obtained.

Decomposition of HMX **30** (δ-phase with the lowest density) was investigated using a new method[217] based on DFT, namely, tight binding molecular dynamics approximation.[218] Theoretical foundations of this method were considered in, *e.g.*, a monograph.[12] A parameterized Hamiltonian was used for calculations. This made it possible to accelerate the calculations by nearly an order of magnitude compared with conventional quantum chemical programmes for calculations of crystals. By fast heating, the periodic cell corresponding to the δ-phase was transferred to the so-called Chapman–Jouget state, *i.e.*, the state in the front of a detonation wave. During recordng of trajectory (55 ps) molecules **30** decomposed to H_2O, CO_2, CO and N_2. Not only the composition of products but also the kinetic data on the decomposition process were obtained. Long simulation time of the decomposition makes its study by quantum chemical methods almost impossible. However, the development of approximate methods of calculations within the framework of DFT allows one to record trajectories whose length is comparable with those obtained by methods using empirical potentials.

Investigations of dynamic processes in crystals require a large amount of computations; therefore, the development of this research avenue is related to progress in hardware. Modern quantum chemical calculations are now used to study vibrational spectra and the nature of disordering of molecules in crystals, as well as the nature of phase transitions not only in simple model crystals, but also in more complex molecular compounds. Quantum chemical calculations of parameters of thermal vibrations are still of limited use. An example of a pioneering study in this field is provided by *a priori* quantum chemical calculations of parameters of thermal vibrations in the crystal of deuterated ammonia (ND_3).[219] One can expect that similar studies will be used for increasingly wider class of molecular crystals and the number of publications concerning dynamic processes in these systems will also increase.

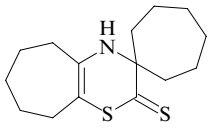
XI. Refinement of structural models used in powder X-ray diffraction

In the last decade, powder X-ray diffraction methods of solution and refinement of the crystal structures of organic and organoelement compounds have been widely used. Unlike inorganic compounds, the structures of organic and organoelement molecules solved and refined using powder X-ray diffraction technique are much less accurate than those determined by single-crystal X-ray diffraction. Structural studies of organic and organoelement compounds can be performed with rigidly fixed geometry of particular molecular fragments (*e.g.*, benzene ring); however, the technique is inapplicable to the coordination polyhedra of metals or conformationally flexible molecules. Quantum chemical calculations with inclusion of the influence of crystal packing can help to refine either initial models obtained during the structure solution process or positions of specified atoms.

An example of refinement of the position of hydrogen atom particpating in the formation of a strong hydrogen bond was reported in the preceding Section (adduct of quadratic acid and 4,4′-bipyridine).[211] Positions of hydrogen atoms were refined in order to calculate solid-state NMR spectra. The structures of naphthalene-2,6-dicarboxylate tetrahydrate salts of cobalt(II) and nickel(II)[220] and terephthalic acid salts $M(C_8H_4O_4)(H_2O)_2$ (M = Mg, Mn, Fe, Co)[221] were refined analogously. Monte Carlo calculations of crystal structures were carried out using diffraction data collected with a synchrotron source. Usually, it is impossible to locate positions of hydrogen atoms from

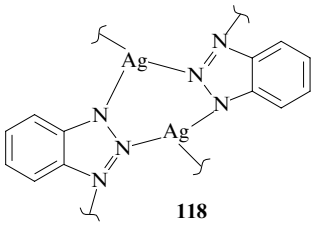
powder diffraction data. Therefore, hydrogen atoms of water molecules were placed in positions established from the results of crystal packing analysis and refined (PW91 functional) with fixed positions of other atoms. Subsequent full optimization [221] showed that the optimized structures do not correspond to the initial models with idealized geometry of molecular fragments. For instance, the coordination polyhedron of the metal atoms was assumed to be structurally similar to an ideal octahedron, which in fact is not the case.

In a study of a complex molecule of compound **117**, quantum chemical calculations (PBE/400 eV) were used to refine the conformations of spirocyclic fragments of two independent molecules in the crystal and to obtain parameters of the hydrogen bond N—H···S.[222]



117

Polymer structure of a benzotriazole complex of silver (**118**) [223] was solved by the Monte Carlo method with some restrictions imposed on the geometry of the benzotriazole fragment. To take into account the influence of packing, the initial model was optimized (programme VASP) and the structure obtained was included in the refinement carried out assuming that only some specified fragments can move relative to one another. A comparison of the calculated (DFT) and final (refined) structures of the complex **118** showed that differences between them are of the order of experimental errors.



118

Application of quantum chemical calculations of crystals to refinement of structural models used in powder X-ray diffraction is a particular case of using computational methods in structural analysis. However, one can also calculate various properties and spectroscopic parameters of the solved and refined structures, which cannot be done in a different way.

* * *

In this review we considered the most important aspects and applications of modern quantum chemical calculations with periodic boundary conditions within the framework of DFT in studies of the structure and properties of molecular crystals of organic and organoelement compounds. Recently, these calculations are increasingly frequently used to solve various physicochemical and crystal chemical problems. This became possible owing to the development and intensive use of new software and high-performance computing facilities whose potential continuously extends to shorten the computing time necessary to perform labour-consuming calculations. We also performed a comparative analysis of the software for quantum chemical calculations and pointed an important role of 'correct' choice of the functional in order to attain good agreement between the experimentally determined and DFT-calculated properties of molecules and crystals. Therefore, one can expect further development of the density functional theory as applied to research on molecular crystals in the nearest future.

The review has been written with the financial support from the Division of Chemistry and Materials Science, Russian Academy of Sciences (Programme OKh-01).

References

1. P Hohenberg, W Kohn *Phys. Rev. B* **136** 864 (1964)
2. W Kohn, L J Sham *Phys. Rev. A* **140** 1133 (1965)
3. J P Perdew, A Zunger *Phys. Rev. B* **23** 5048 (1981)
4. S Vosko, L Wilk, M Nusair *Can. J. Phys.* **58** 1200 (1980)
5. C Lee, W Yang, R G Parr *Phys. Rev. B* **37** 785 (1988)
6. A D Becke *Phys. Rev. A* **38** 3098 (1988)
7. J P Perdew *Phys. Rev. B* **33** 8822 (1986)
8. J P Perdew, Y Wang *Phys. Rev. B* **45** 13244 (1992)
9. J P Perdew, K Burke, M Ernzerhof *Phys. Rev. Lett.* **77** 3865 (1996)
10. J P Perdew, S Kurth, A Zupan, P Blaha *Phys. Rev. Lett.* **82** 2544 (1999)
11. A D Becke *J. Chem. Phys.* **98** 5648 (1993)
12. R M Martin *Electronic Structure: Basic Theory and Practical Methods* (Cambridge: Cambridge University Press, 2004)
13. V G Tsirelson *Kvantovaya Khimiya. Molekuly, Molekulyarnye Sistemy i Tverdye Tela* (Quantum Chemistry. Molecules, Molecular Systems and Solids) (Moscow: Binom, 2010)
14. R Ditchfield, W J Hehre, J A Pople *J. Chem. Phys.* **54** 724 (1971)
15. W J Hehre, R Ditchfield, J A Pople *J. Chem. Phys.* **56** 2257 (1972)
16. G te Velde, E J Baerends *Phys. Rev. B* **44** 7888 (1991)
17. J C Slater *Phys. Rev.* **51** 846 (1937)
18. D Vanderbilt *Phys. Rev. B* **41** 7892 (1990)
19. P E Bloechl *Phys. Rev. B* **50** 17953 (1994)
20. G Kresse, D Joubert *Phys. Rev. B* **59** 1758 (1999)
21. A S Fedorov, P B Sorokin, P V Avramov, S G Ovchinnikov *Modelirovanie Svoistv Elektronnoi Struktury Ryada Uglerodnykh i Neuglerodnykh Nanoklasterov i ikh Vzaimodeistvie s Legkimi Elementami* (Modelling of Electronic Structure Properties of some Carbon and Noncarbon Nanoclusters and Their Interaction with Light Elements) (Novosibirsk: Siberian Branch of the Russian Academy of Sciences, 2006)
22. M Schmidt, K Balridge, J Boatz, S Elbert, M Gordon, J Jensen, S Koseki, N Matsunaga, K Nguyen, S Su, T Windus, M Dupuis, J Montgomery *J. Comput. Chem.* **14** 1347 (1993)
23. M J Frisch, G W Trucks, H B Schlegel, G E Scuseria, M A Robb, J R Cheeseman, J Montgomery, T Vreven, K N Kudin, J C Burant, J M Millam, S S Iyengar, J Tomasi, V Barone, B Mennucci, M Cossi, G Scalmani, N Rega, G A Petersson, H Nakatsuji, M Hada, M Ehara, K Toyota, R Fukuda, J Hasegawa, M Ishida, T Nakajima, Y Honda, O Kitao, H Nakai, M Klene, X Li, J E Knox, H P Hratchian, J B Cross, V Bakken, C Adamo, J Jaramillo, R Gomperts, R E Stratmann, O Yazyev, A J Austin, R Cammi, C Pomelli, J W Ochterski, P Y Ayala, K Morokuma, G A Voth, P Salvador, J J Dannenberg, V G Zakrzewski, S Dapprich, A D Daniels, M C Strain, O Farkas, D K Malick, A D Rabuck, K Raghavachari, J B Foresman, J V Ortiz, Q Cui, A G Baboul, S Clifford, J Cioslowski, B B Stefanov, G Liu, A Liashenko, P Piskorz, I Komaromi, R L Martin D J Fox, T Keith, M A Al-Laham, C Y Peng, A Nanayakkara, M Challacombe, P M W Gill, B Johnson, W Chen, M W Wong, C Gonzalez, J A Pople *Gaussian 03 C.01* Gaussian Inc. Pittsburgh, 1998

24. S B Andrews, N A Burton, I H Hilier, J M Holender, M J Gillan *Chem. Phys. Lett*. **261** 521 (1996)
25. R J Meier *J. Mol. Struct. (THEOCHEM)* **467** 79 (1999)
26. G Lippert, J Hutter, M Parrinello *Theor. Chim. Acta* **103** 124 (1999)
27. C Massobrio, E Ruiz *Monatsh. Chem*. **134** 317 (2003)
28. S Tosoni, C Tuma, J Sauer, B Civalleri, P Ugliengo *J. Chem. Phys*. **127** 154102 (2007)
29. J Hafner *J. Comput. Chem*. **29** 2044 (2008)
30. J Vande Vondele, M Krack, F Mohamed, M Parrinello, T Chassaing, J Hutter *Comput. Phys. Commun*. **167** 103 (2005)
31. P Blaha, K Schwarz, G K H Madsen, D Kvasnicka, J Luitz *WIEN2k, An Augmented Plane Wave + Local Orbitals Program for Calculating Crystal Properties* (Wien: Technische Universitit, 2001)
32. N Troullier J L Martins *Phys. Rev. B* **43** 1993 (1991)
33. S J Clark, M D Segall, C J Pickard, P J Hasnip, M J Probert, K Refson, M C Payne *Z. Kristallogr*. **220** 567 (2005)
34. B Delley *J. Chem. Phys*. **113** 7756 (2000)
35. G Kresse, J Furthmuller *Phys. Rev. B* **54** 11169 (1996)
36. G Kresse, J Hafner *Phys. Rev. B* **47** 558 (1993)
37. G Kresse, J Furthmuller *Comput. Mater. Sci*. **6** 15 (1996)
38. W Adreoni A Curioni *Parallel Comput*. **26** 819 (2000)
39. R Dovesi, B Orlando, B Civalleri, R Roetti, V R Saunders, C M Zicovich-Wilson *Z. Kristallogr*. **220** 571 (2005)
40. P Giannozzi, S Baroni, N Bonini, M Calandra, R Car, C Cavazzoni, D Ceresoli, G L Chiarotti, M Cococcioni, I Dabo, A Dal Corso, S de Gironcoli, S Fabris, G Fratesi, R Gebauer, U Gerstmann, C Gougoussis, A Kokalj, M Lazzeri, L Martin-Samos, N Marzari, F Mauri, R Mazzarello, S Paolini, A Pasquarello, L Paulatto, C Sbraccia, S Scandolo, G Sclauzero, A P Seitsonen, A Smogunov, P Umari, R M Wentzcovitch *J. Phys.: Condens. Matter* **21** 395502 (2009)
41. J M Soler, E Artacho, J D Gale, A Garcta, J Junquera, P Ordejdn, D Svnchez-Portal *J. Phys.: Condens. Matter* **14** 2745 (2002)
42. M A Neumann, M Perrin *J. Phys. Chem. B* **109** 15531 (2005)
43. E F C Byrd, G E Scuseria, C F Chabalowski *J. Phys. Chem. B* **108** 13100 (2004)
44. E F Byrd, B M Rice *J. Phys. Chem. C* **111** 2787 (2007)
45. F Pichierri, A Sekine, T Ebisuzaki *Chem. Phys. Lett*. **264** 9 (2001)
46. K Nagayoshi, K Kitaura, S Koseki, S Re, K Kobayashi, Y Choe, S Nagase *Chem. Phys. Lett*. **369** 597 (2003)
47. J C Collings, K P Roscoe, E G Robins, A S Batsanov, L M Stimson, J A Howard, S J Clark, T B Marder *New J. Chem*. **26** 1740 (2002)
48. C E Smith, P S Smith, R L Thomas, E G Robins, J C Collings, C Dai, A J Scott, S Borwick, A S Batsanov, S W Watt, S J Clark, C Viney, J A K Howard, W Clegg, T B Marder *J. Mater. Chem*. **14** 413 (2004)
49. K A Lyssenko, A A Korlyukov, D G Golovanov, S Y Ketkov, M Yu Antipin *J. Phys. Chem. A* **110** 6545 (2006)
50. K A Lyssenko, A A Korlyukov, M Yu Antipin *Mendeleev Commun*. 90 (2005)
51. R H Boyd *Tetrahedron* **22** 119 (1966)
52. D L Rodgers, E F Westrum Jr, J T S Andrews *J. Chem. Thermodyn*. **5** 733 (1973)
53. J A Connor, H A Skinner, Y Virmani *J. Chem. Soc., Faraday Trans*. **69** 1218 (1973)
54. I V Glukhov, K A Lyssenko, A A Korlyukov, M Yu Antipin *Izv. Akad. Nauk, Ser. Khim*. 541 (2005) [a]
55. A D Dilman, D E Arkhipov, A A Korlyukov, V P Ananikov, V M Danilenko, V A Tartakovsky *J. Organomet. Chem*. **690** 3680 (2005)
56. A Hu, B Larade, S Dudiy, H Abou-Rachid, L Lussier, H Guo *Prop. Explos. Pyrotech*. **32** 331 (2007)
57. B Civalleri, K Doll, C M Zicovich-Wilson *J. Phys. Chem. B* **111** 26 (2007)
58. J P Perdew, A Ruzsinszky, G I Csonka, O A Vydrov, G E Scuseria, L A Constantin, X Zhou, K Burke *Phys. Rev. Lett*. **100** 136406 (2008)
59. R Armiento, A E Mattsson *Phys. Rev. B* **72** 085108 (2005)
60. Y Zhao, D G Truhlar *J. Phys. Chem. A* **109** 5656 (2005)
61. J Moellmann, S Grimme *Phys. Chem. Chem. Phys*. **12** 8500 (2010)
62. R W Williams, D Malhotra *Chem. Phys*. **327** 54 (2006)
63. S Grimme *J. Comput. Chem*. **27** 1787 (2006)
64. E J Meijer, M Sprik *J. Chem. Phys*. **105** 8684 (1996)
65. M Bernasconi, M Parrinello, G L Chiarotti, P Focher, E Tosatti *Phys. Rev. Lett*. **76** 2081 (1996)
66. K E Riley, M Pitoňák, P Jurečka, P Hobza *Chem. Rev*. **110** 5023 (2010)
67. M W Conroy, I I Oleynik, S V Zybin, C T White *J. Phys. Chem. A* **113** 3610 (2009)
68. G L Perlovich, T V Volkova, A Bauer-Brandl *J. Pharm. Sci*. **95** 2158 (2006)
69. H Wiedemann *Thermochim. Acta* **3** 355 (1972)
70. Y Ohta, A Demura, T Okamoto, H Hitomi, M Nagaoka *J. Phys. Chem. B* **110** 12640 (2006)
71. J D Dunitz, A Gavezzotti *Chem. Soc. Rev*. **38** 2622 (2009)
72. J Bernstein *Polymorphism in Molecular Crystals* (Oxford: Clarendon Press, 2002)
73. J D Gale, A L Rohl *Mol. Simul*. **29** 291 (2003)
74. J D Gale *Faraday Trans*. **93** 629 (1997)
75. B P van Eijick, W T Mooij, J Kroon *Acta Crystallogr., Sect. B* **51** 99 (1995)
76. M A Neumann, F Leusen, J Kendrick *Angew. Chem., Int. Ed*. **47** 2427 (2008)
77. C Rovira, J J Novoa *J. Phys. Chem. B* **105** 1710 (2001)
78. R Boese, D Bläser, R Latz, A Biumen *Acta Crystallogr., Sect. C* **55** 9900001 (1999)
79. D R Allan, S J Clark *Phys. Rev. B* **60** 6328 (1999)
80. R Boese, A J Downs, T M Greene, A W Hall, C A Morrison, S Parsons *Organometallics* **22** 2450 (2003)
81. J A Chisholm, S Motherwell, P R Tulip, S Parsons, S J Clark *Cryst. Growth Des*. **5** 1437 (2005)
82. C M Freeman, J W Andzelm, C S Ewig, J Hill, B Delley *Chem. Commun*. 2455 (1998)
83. S A Rivera, D G Allis, B S Hudson *Cryst. Growth Des*. **8** 3905 (2008)
84. D M S Martins, C K Spanswick, D S Middlemiss, N Abbas, C R Pulham, C A Morrison *J. Phys. Chem. A* **113** 5998 (2009)
85. K Hongo, M A Watson, R S Sánchez-Carrera, T Iitaka, A Aspuru-Guzik *J. Phys. Chem. Lett*. **1** 1789 (2010)
86. A Brillante, R G Della Valle, L Farina, E Venuti, C Cavazzoni, A P J Emerson, K Syassen *J. Am. Chem. Soc*. **127** 3038 (2005)
87. T Lin, X Y Liu, C He *Polymer* **51** 2779 (2010)
88. J Hernandez-Paredes, D Glossman-Mitnik, H E Esparza-Ponce, M E Alvarez-Ramos, A Duarte-Moller *J. Mol. Struct*. **875** 295 (2008)
89. J P Zou, G S Zeng, Z H Wen, Q Peng, Q J Xing, M H Chen, G C Guo, J S Huang *Inorg. Chim. Acta* **362** 4843 (2009)
90. Y H Liu, Y Xie, Z Y Lu *Chem. Phys*. **367** 160 (2009)
91. R S Sánchez-Carrera, V Coropceanu, E Kim, J Brgdas *Chem. Mater*. **20** 5832 (2008)
92. G-W An, H Zhang, X-L Cheng, Q-L Zhuo, Y-C Lv *Struct. Chem*. **19** 613 (2008)
93. G A de Wijs, C C Mattheus, R A de Groot, T Palstra *Synth. Met*. **139** 109 (2003)
94. M C Delgado, K R Pigg, D A da Silva Filho, N E Gruhn, Y Sakamoto, T Suzuki, R M Osuna, J Casado, V Hernvndez, J T Navarrete *J. Am. Chem. Soc*. **131** 1502 (2009)
95. S Salman, M C Delgado, V Coropceanu, J L Brédas *Chem. Mater*. **21** 3593 (2009)
96. E G Kim, J L Brédas *J. Am. Chem. Soc* **130** 16880 (2008)
97. M C R Delgado, E G Kim, D A D S Filho, J L Brédas *J. Am. Chem. Soc*. **132** 3375 (2010)
98. A H Reshak, D Stys, S Auluck, I V Kityk *J. Phys. Chem. B* **113** 12648 (2009)

99. P X Li, H L Jiang, M L Feng, J G Mao *Inorg. Chem.* **46** 8302 (2007)
100. Y Li, G Zheng, C Lin, J Lin *Solid State Sci.* **9** 855 (2007)
101. D S Middlemiss, L M Lawton, C A Morrison, C C Wilson *Chem. Phys. Lett.* **459** 119 (2008)
102. A E Reed, L A Curtiss, F Weinhold *Chem. Rev.* **88** 899 (1988)
103. F Weinhold, C R Landis *A Natural Bond Orbital Donor-Acceptor Perspectives* (Madison, WI: University of Wisconsin, 2005)
104. R F W Bader *Atoms in Molecules: A Quantum Theory* (New York: Oxford University Press, 1990)
105. F W Biegler-König, R F W Bader, T Tang *J. Comput. Chem.* **3** 317 (1982)
106. F Biegler-König, J Schönbohm, D Bayles *J. Comput. Chem.* **22** 545 (2001)
107. P L A Popelier *Comput. Phys. Commun.* **93** 212 (1996)
108. S Noury, X Krokidis, F Fuster, B Silvi *Comput. Chem.* **23** 597 (1999)
109. T A Keith *AIMALL* version 09.04.23; http://aim.tkgristmill.com
110. A Volkov, T Koritsanszky, M Chodkiewicz, H F King *J. Comput. Chem.* **30** 1379 (2009).
111. L Bertini, F Cargnoni, C Gatti *Theor. Chim. Acta* **117** 847 (2007)
112. N K Hansen P Coppens *Acta Crystallogr., Sect. A* **34** 909 (1978)
113. A Volkov, P Macchi, L J Farrugia, C Gatti, P Mallinson, T Richter, T Koritzansky *XD2006 — A Computer Program Package for Multipole Refinement, Topological Analysis of Charge Densities and Evaluation of Intermolecular Energies from Experimental and Theoretical Structure Factors, 2006*
114. H Brunning, D Feil *Acta Crystallogr., Sect. A* **48** 865 (1992)
115. R Y Vries, D Feil, V G Tsirelson *Acta Crystallogr., Sect. B* **56** 118 (2000)
116. M Kohout *Programs DGrid and Basin*; http://www.cpfs.mpg.de/~kohout/dgrid.html
117. X Gonze, J-M Beuken, R Caracas, F Detraux, M Fuchs, G-M Rignanese, L Sindic, M Verstraete, G Zerah, F Jollet, M Torrent, A Roy, M Mikami, P Ghosez, J-Y Raty, D C Allan *Comput. Mater. Sci.* **25** 478 (2002)
118. W Tang, E Sanville, G Henkelman *J. Phys.: Condens. Matter* **21** 084204 (2009)
119. C Katan, P Rabilier, C Lecomte, M Guezo, V Oison, M Souhassou *J. Appl. Crystallogr.* **36** 65 (2003)
120. Y Aray, J Rodriguez, R Lopez-Boada *J. Phys. Chem. A* **101** 2178 (1997)
121. W Yim, T Klüner *J. Comput. Chem.* **29** 1306 (2008)
122. R F W Bader, R J Gillespie, F Martín *Chem. Phys. Lett.* **290** 488 (1998)
123. J Cioslowski, P Piskorz *Chem. Phys. Lett.* **255** 315 (1996)
124. S F Vyboishchikov, A Sierraalta, G Frenking *J. Comput. Chem.* **18** 416 (1997)
125. M Hô, H Schmider, K E Edgecombe, V H Smith Jr *Int. J. Quant. Chem.* **52** (S28) 215 (1994)
126. A A Korlyukov, M Yu Antipin, Yu I Bolgova, O M Trofimova, M G Voronkov *Izv. Akad. Nauk, Ser. Khim.* 25 (2009) [a]
127. A A Korlyukov, M Yu Antipin, M I Buzin, E A Zel'bst, Yu I Bolgova, O M Trofimova, M G Voronkov *Zh. Strukt. Khim.* 911 (2009) [b]
128. V V Levin, A D Dilman, A A Korlyukov, P A Belyakov, M I Struchkova, M Yu Antipin, V A Tartakovsky *Izv. Akad. Nauk, Ser. Khim.* 1345 (2007) [a]
129. A A Korlyukov, K A Lyssenko, M Yu Antipin, E A Grebneva, A I Albanov, O M Trofimova, E A Zel'bst, M G Voronkov *J. Organomet. Chem.* **694** 607 (2009)
130. I A Tikhonova, K I Tugashov, F M Dolgushin, A A Korlyukov, P V Petrovskii, Z S Klemenkova, V B Shur *J. Organomet. Chem.* **694** 2604 (2009)
131. L S Alekseev, A V Safronov, F M Dolgushin, A A Korlyukov, I A Godovikov, I T Chizhevsky *J. Organomet. Chem.* **694** 1727 (2009)
132. E A Komissarov, A A Korlyukov, E P Kramarova, S Y Bylikin, V V Negrebetsky, Y I Baukov *Acta Crystallogr., Sect. C* **63** m144 (2007)
133. A A Korlyukov, E A Komissarov, M Yu Antipin, N V Alekseev, K V Pavlov, O V Krivolapova, V G Lahtin, E A Chernyshev *J. Mol. Struct.* **875** 135 (2008)
134. A D Dilman, V V Levin, A A Korlyukov, P A Belyakov, M I Struchkova, M Yu Antipin, V A Tartakovsky *J. Organomet. Chem.* **693** 1005 (2008)
135. A A Korlyukov, S A Pogozhikh, Yu E Ovchinnikov, K A Lyssenko, M Yu Antipin, A G Shipov, O A Zamyshlyaeva, E P Kramarova, V V Negrebetsky, I P Yakovlev, Yu I Baukov *J. Organomet. Chem.* **691** 3962 (2006)
136. A O Borissova, A A Korlyukov, M Yu Antipin, K A Lyssenko *J. Phys. Chem. A* **112** 11519 (2008)
137. E Espinosa, E Molins, C Lecomte *Chem. Phys. Lett.* **285** 170 (1998)
138. E Espinosa, C Lecomte, E Molins *Chem. Phys. Lett.* **300** 745 (1999)
139. E Espinosa, I Alkorta, I Rozas, J Elguero, E Molins *Chem. Phys. Lett.* **336** 457 (2001)
140. I F Shishkov, L V Khristenko, F M Rudakov, A B Golubinskii, L V Vilkov, S S Karlov, G S Zaitseva, S Samdal *Struct. Chem.* **15** 11 (2004)
141. G Forgvcs, M Kolonits, I Hargittai *Struct. Chem.* **1** 245 (1990)
142. M V Zabalov, S S Karlov, G S Zaitseva, D A Lemenovskii *Izv. Akad. Nauk, Ser. Khim.* 448 (2006) [a]
143. A Bondi *J. Phys. Chem.* **68** 441 (1964)
144. E May, R Destro, C Gatti *J. Am. Chem. Soc.* **123** 12248 (2001)
145. M V Vener, A V Manaev, A N Egorova, V G Tsirelson *J. Phys. Chem. A* **111** 1155 (2007)
146. P Munshi, C Jelsch, V R Hathwar, T N Guru Row *Cryst. Growth Design.* **10** 1516 (2010)
147. J Ellena, A E Goeta, J A K Howard, G Punte *J. Phys. Chem. A* **105** 8696 (2001)
148. L J Farrugia, C Evans, D Lentz, M Roemer *J. Am. Chem. Soc.* **131** 1251 (2009)
149. L J Farrugia, H M Senn *J. Phys. Chem. A* **114** 13418 (2010)
150. R K Harris, R E Wasylishen, M J Duer *NMR Crystallography* (Singapore: Wiley, 2009)
151. C G Van de Walle, P E Blöchl *Phys. Rev. B* **47** 4244 (1993)
152. F Mauri, A Pasquarello, B G Pfrommer, Y Yoon, S G Louie *Phys. Rev. B* **62** R4786 (2000)
153. J Schmidt, A Hoffmann, H W Spiess, D Sebastiani *J. Phys. Chem. B* **110** 23204 (2006)
154. D Sebastiani, G Goward, I Schnell, H W Spiess *J. Mol. Struct. (THEOCHEM)* **625** 283 (2003)
155. C J Pickard, F Mauri *Phys. Rev. B* **63** 245101 (2001)
156. R K Harris, P Hodgkinson, C J Pickard, J R Yates, V Zorin *Magn. Reson. Chem.* **45** S174 (2007)
157. V Milman, K Refson, S Clark, C Pickard, J Yates, S Gao, P Hasnip, M Probert, A Perlov, M Segall *J. Mol. Struct. (THEOCHEM)* **954** 22 (2010)
158. J C Johnston, R J Iuliucci, J C Facelli, G Fitzgerald, K T Müller *J. Chem. Phys.* **131** 144503 (2009)
159. J Dumez, C J Pickard *J. Chem. Phys.* **130** 104701 (2009)
160. J R Yates, S E Dobbins, C J Pickard, F Mauri, P Y Ghi, R K Harris *Phys. Chem. Chem. Phys.* **7** 1402 (2005)
161. A J Robbins, W T K Ng, D Jochym, T W Keal, S J Clark, D J Tozer, P Hodgkinson *Phys. Chem. Chem. Phys.* **9** 2389 (2007)
162. R K Harris, S Cadars, L Emsley, J R Yates, C J Pickard, R K R Jetti, U J Griesser *Phys. Chem. Chem. Phys.* **9** 360 (2007)

163. E Salager, R S Stein, C J Pickard, B Elena, L Emsley *Phys. Chem. Chem. Phys.* **11** 2610 (2009)
164. A C Uldry, J M Griffin, J R Yates, M Pérez-Torralba, M D Santa María, A L Webber, M L Beaumont, A Samoson, R M Claramunt, C J Pickard *J. Am. Chem. Soc* **130** 945 (2008)
165. I Hung, A Uldry, J Becker-Baldus, A L Webber, A Wong, M E Smith, S A Joyce, J R Yates, C J Pickard, R Dupree, S P Brown *J. Am. Chem. Soc.* **131** 1820 (2009)
166. C Gervais, R Dupree, K J Pike, C Bonhomme, M Profeta, C J Pickard, F Mauri *J. Phys. Chem. A* **109** 6960 (2005)
167. A Zheng, S Liu, F Deng *J. Comput. Chem.* **30** 222 (2009)
168. A Dos, V Schimming, S Tosoni, H Limbach *J. Phys. Chem. B* **112** 15604 (2008)
169. J R Yates, T N Pham, C J Pickard, F Mauri, A M Amado, A M Gil, S P Brown *J. Am. Chem. Soc.* **127** 10216 (2005)
170. L Seyfarth, J Sehnert, N E A El-Gamel, W Milius, E Kroke, J Breu, J Senker *J. Mol. Struct.* **889** 217 (2008)
171. R K Harris, P Y Ghi, R B Hammond, C Y Ma, K J Roberts, J R Yates, C J Pickard *Magn. Reson. Chem.* **44** 325 (2006)
172. E Salager, G M Day, R S Stein, C J Pickard, B Elena, L Emsley *J. Am. Chem. Soc.* **132** 2564 (2010)
173. J R Yates, C J Pickard, M C Payne, R Dupree, M Profeta, F Mauri *J. Phys. Chem. A* **108** 6032 (2004)
174. C Gervais, L Bonhomme-Coury, F Mauri, F Babonneau, C Bonhomme *Phys. Chem. Chem. Phys.* **11** 6953 (2009)
175. C Gervais, M Profeta, V Lafond, C Bonhomme, T Azaïs, H Mutin, C J Pickard, F Mauri, F Babonneau *Magn. Reson. Chem.* **42** 445 (2004)
176. K Parlinski, in *Conference Proceedings 479 'Neutrons and Numerical Methods N2M', Grenoble, 1999* p. 121
177. J A Zeitler, P F Taday, D A Newnham, M Pepper, K C Gordon, T Rades *J. Pharm. Pharmacol.* **59** 209 (2007)
178. P Jepsen, D Cooke, M Koch *Laser Photon. Rev.* **5** 124 (2011)
179. S L Dexheimer *Terahertz Spectroscopy: Principles and Applications* (New York: CRC Press, 2007)
180. J A Ciezak, S F Trevino *J. Mol. Struct. (THEOCHEM)* **723** 241 (2005)
181. M Plazanet, N Fukushima, M R Johnson *Chem. Phys.* **280** 53 (2002)
182. C C Wilson, C A Morrison *Chem. Phys. Lett.* **362** 85 (2002)
183. L van Eijck, M R Johnson, G J Kearley *J. Phys. Chem. A* **107** 8980 (2003)
184. P Hermet, J Bantignies, A Rahmani, J Sauvajol, M R Johnson, F Serein *J. Phys. Chem. A* **109** 1684 (2005)
185. M Plazanet, M R Johnson, J D Gale, T Yildirim, G J Kearley, M T Fernández-Díaz, D Sánchez-Portal, E Artacho, J M Soler, P Ordejón *Chem. Phys.* **261** 189 (2000)
186. J A Ciezak, S F Trevino *J. Phys. Chem. A* **110** 5149 (2006)
187. M R Hudson, D G Allis, B S Hudson *J. Phys. Chem. A* **114** 3630 (2010)
188. B S Hudson, D A Braden, D G Allis, T Jenkins, S Baronov, C Middleton, R Withnall, C M Brown *J. Phys. Chem. A* **108** 7356 (2004)
189. A Trivella, T Gaillard, R H Stote, P Hellwig *J. Chem. Phys.* **132** 115105 (2010)
190. J Eckert, T D Sewell, J D Kress, E M Kober, L L Wang, G Olah *J. Phys. Chem. A* **108** 11369 (2004)
191. Y U Paulechka, G J Kabo, A V Blokhin, A S Shaplov, E I Lozinskaya, D G Golovanov, K A Lyssenko, A A Korlyukov, Y S Vygodskii *J. Phys. Chem. B* **113** 9538 (2009)
192. P Hermet, J Bantignies, A Rahmani, J Sauvajol, M R Johnson *J. Phys. Chem. A* **109** 4202 (2005)
193. D Marx, J Hutter *Mod. Meth. Algor. Quant. Chem.* **1** 301 (2000)
194. B S Hudson, J S Tse, M Z Zgierski, S F Parker, D A Braden, C Middleton *Chem. Phys.* **261** 249 (2000)
195. M R Johnson, H P Trommsdorff *Chem. Phys. Lett.* **364** 34 (2002)
196. M D King, P M Hakey, T M Korter *J. Phys. Chem. A* **114** 2945 (2010)
197. P M Hakey, D G Allis, M R Hudson, W Ouellette, T M Korter *J. Phys. Chem. A* **114** 4364 (2010)
198. P U Jepsen, S J Clark *Chem. Phys. Lett.* **442** 275 (2007)
199. M Takahashi, Y Kawazoe, Y Ishikawa, H Ito *Chem. Phys. Lett.* **479** 211 (2009)
200. A D Burnett, J Kendrick, J E Cunningham, M D Hargreaves, T Munshi, H G Edwards, E H Linfield, A G Davies *Chem. Phys. Chem* **11** 368 (2010)
201. M D King, W D Buchanan, T M Korter *Phys. Chem. Chem. Phys.* **13** 4250 (2011)
202. Ya S Vygodskii, O A Mel'nik, E I Lozinskaya, A S Shaplov, I A Malyshkina, N D Gavrilova, K A Lyssenko, M Yu Antipin, D G Golovanov, A A Korlyukov, N Ignat'ev, U Welz-Biermann *Polym. Adv. Technol.* **18** 50 (2007)
203. C A Morrison, D S Wright, R A Layfield *J. Am. Chem. Soc.* **124** 6775 (2002)
204. I I Vorontsov, K A Potekhin, M Yu Antipin, I E Zanin *Kristallografiya* **45** 266 (2000) [c]
205. K A Lyssenko, M Yu Antipin, S Yu Ketkov *Izv. Akad. Nauk, Ser. Khim.* 130 (2001)
206. P Seiler, J D Dunitz *Acta Crystallogr., Sect. B* **35** 1068 (1979)
207. M Yu Antipin, R Boese *Acta Crystallogr., Sect. B* **52** 314 (1996)
208. C C Wilson, L H Thomas, C A Morrison *Chem. Phys. Lett.* **381** 102 (2003)
209. R Boese, M Y Antipin, D Blaser, K A Lyssenko *J. Phys. Chem. B* **102** 8654 (1998)
210. M V Vener, A V Manaev, V G Tsirelson *J. Phys. Chem. A* **112** 13628 (2008)
211. D M Martins, D S Middlemiss, C R Pulham, C C Wilson, M T Weller, P F Henry, N Shankland, K Shankland, W G Marshall, R M Ibberson *J. Am. Chem. Soc.* **131** 3884 (2009)
212. M V Vener, N B Librovich *Int. Rev. Phys. Chem.* **28** 407 (2009)
213. C A Morrison, M M Siddick, P J Camp, C C Wilson *J. Am. Chem. Soc.* **127** 4042 (2005)
214. A Jezierska-Mazzarello, R Vuilleumier, J J Panek, G Ciccotti *J. Phys. Chem. B* **114** 242 (2010)
215. M E Tuckerman, M L Klein *Chem. Phys. Lett.* **283** 147 (1998)
216. A C Landerville, I I Oleynik, C T White *J. Phys. Chem. A* **113** 12094 (2009)
217. M R Manaa, L E Fried, C F Melius, M Elstner, T Frauenheim *J. Phys. Chem. A* **106** 9024 (2002)
218. D Porezag, T Frauenheim, T Köhler, G Seifert, R Kaschner *Phys. Rev. B: Condens. Matter* **51** 12947 (1995)
219. A M Reilly, S Habershon, C A Morrison, D W H Rankin *J. Chem. Phys.* **132** 134511 (2010)
220. J A Kaduk, J A Hanko *J. Appl. Crystallogr.* **34** 710 (2001)
221. J A Kaduk *Acta Crystallogr., Sect. B* **58** 815 (2002)
222. E E Avila, A J Mora, G E Delgado, R R Contreras, A N Fitch, M Brunelli *Acta Crystallogr., Sect. B* **64** 217 (2008)
223. M Rajeswaran, T N Blanton, D J Giesen, D R Whicomb, N Zumbulyadis, B J Antalek, M M Neumann, S T Misture *J. Solid State Chem.* **179** 1053 (2006)

[a] — *Russ. Chem. Bull., Int. Ed. (Engl. Transl.)*
[b] — *J. Struct. Chem. (Engl. transl.)*
[c] — *Crystallogr. Rep. (Engl. Transl.)*